III

Theoretical Modeling of the Heme Group with a Hybrid QM/MM Method

Jean-Didier Maréchal, Guada Barea, Feliu Maseras, Agustí Lledós, Feliu Maseras, Liliane Mouawad and David Pérahia

Unitat de Química Física, Edifici C.n, Universitat Autònoma e Barcelona, 08193 Bellaterra, Catalonia, Spain. Laboratoire de Modélisation et Ingénierie des Protéines, Bât 430, Université de Paris Sud, 91405 Orasy, Cedex, France.

Journal of Computational Chemistry®

2000 Volume 21, Number 4, Pages 282-294

Theoretical Modeling of the Heme Group with a Hybrid QM/MM Method

JEAN-DIDIER MARÉCHAL,[1,2] GUADA BAREA,[1] FELIU MASERAS,[1] AGUSTÍ LLEDÓS,[1] LILIANE MOUAWAD,[2] DAVID PÉRAHIA[2]

[1]*Unitat de Química Física, Edifici C.n, Universitat Autònoma de Barcelona, 08193 Bellaterra, Catalonia, Spain*

[2]*Laboratoire de Modélisation et Ingénierie des Protéines, Bât 430, Université de Paris Sud, 91405 Orsay, Cedex, France*

Received 8 July 1999; accepted 18 October 1999

ABSTRACT: The quality of the results obtained in calculations with the hybrid QM/MM method IMOMM on systems where the heme group is partitioned in QM and MM regions is evaluated through the performance of calculations on the 4-coordinate [Fe(P)] (P = porphyrin), the 5-coordinate [Fe(P)(1 − (Me)Im)] (Im = imidazole) and the 6-coordinate [Fe(P)(1 − (Me)Im)(O_2)] systems. The results are compared with those obtained from much more expensive pure quantum mechanics calculations on model systems. Three different properties are analyzed—namely, the optimized geometries, the binding energies of the axial ligands to the heme group, and the energy cost of the biochemically relevant out-of-plane displacement of the iron atom. Agreement is especially good in the case of optimized geometries and energy cost of out-of-plane displacements, with larger discrepancies in the case of binding energies. © 2000 John Wiley & Sons, Inc. J Comput Chem 21: 282–294, 2000

Keywords: IMOMM method; hybrid QM/MM methods; heme group; iron porphyrin complexes; bioinorganic chemistry

Correspondence to: F. Maseras; e-mail: feliu@klingon.uab.es

Contract/grant sponsor: Training and Mobility of Research program; contract/grant number: ERBFMBICT97-056

Contract/grant sponsor: Spanish DGES; contract/grant number: PB98-0916-CO2-01

Introduction

The heme group occupies a prominent position in biochemistry. It is in the active center of a number of very relevant proteins. Among these, there are the oxygen transport proteins hemoglobin and myoglobin,[1] as well as enzymes involved in catabolism as peroxidases,[2] catalases, oxidases,[3] and cytochromes.[4] Furthermore, other very relevant groups are structurally related to heme. The replacement of Fe by Mg leads to chlorophyll;[5] and replacement of the metal by other transition metals coupled with modifications in the aromatic ring, leads to species as vitamin B_{12}[6] and cofactor F-430.[7] It is, thus, no wonder that the study of bioinorganic models of the heme group has been a focal point of experimental bioinorganic chemistry for years.[8]

Experimental characterization of the reactivity of the heme group appears, however, as challenging. Its versatility, which is probably the key to its biochemical activity, makes experimental isolation of active species very difficult. Because of that, the heme group is an appealing target for theoretical methods. There are indeed a number of studies. One can cite in this concern the early works by Rohmer, Dedieu, and coworkers on the characterization of the electronic state of Fe(P) (P = porphyrin) complexes,[9] where they could predict an electronic structure that was later on proved by experiment.[10] There are also a number of issues where theoretical studies are having an impact on the ongoing discussion, as the real position of the CO group in [Fe(P)(imidazole)(CO)] complexes,[11, 12] the role of distal and proximal histidines on the binding of oxygen in hemoglobin,[13–15] or structural aspects of the binding of dioxygen and other ligands to heme substrates.[16, 17] The amount of information that can be obtained from the calculations is, however, seriously limited by the size of the heme group itself, with its 24-s period atoms, which poses a very serious strain in the computational demand, and that has allowed only recently the appearance of theoretical studies on reactivity.[18–20]

Hybrid QM/MM methods are currently emerging as a powerful tool for the quantitative study of large systems. In these methods, the system is partitioned in different regions, with the higher level method being applied only to the region where it is required. In this way the computational effort of the calculation can be dramatically reduced, and, if the partition is appropriately chosen, the results are practically unchanged. We have already applied one of these methods, IMOMM,[21] to a number of transition metal systems with success.[22]

Application of this kind of methods to the modeling of heme groups raises the question of the validity of introducing a QM/MM partition *within* the porphyrin ring. The fact that the four nitrogen donor atoms of the porphyrin are part of a large aromatic ring has obviously two types of effects on the complex. One of them is the existence of a quite rigid framework, which, among other things, precludes distortions towards a tetrahedral arrangement. This effect can be well reproduced in IMOMM calculations. The second effect concerns the electronic possibilities of the porphyrin ring as an electronic reservoir where the occupied and empty orbitals are relatively close. This effect will be poorly reproduced in IMOMM calculations. Some available data on pure QM calculations with $[Fe(NH(CH)_3NH)_2]$ models,[23] as well as a preliminary IMOMM study on Fe(P)(imidazole)(O_2) look nevertheless promising.[24]

The current article presents a systematic study of the performance of the IMOMM method on a series of systems involving the heme group. These are the 4-coordinate [Fe(P)] system, the 5-coordinate [Fe(P)(Im)] system, and the 6-coordinate [Fe(P)(Im)(O_2)] system. For each of these systems, a series of properties are studied, the focus being in the comparison of the IMOMM results with those of much more expensive full QM calculations. After the computational details, a section follows on each of the three coordination modes. An additional section analyzes the results of a pure QM optimization of the QM region of the IMOMM calculation. Afterwards, the computational level used for the QM part is briefly discussed, and a final section collects the conclusions.

Computational Details

Pure quantum mechanics calculations are performed with the Gaussian 94 program.[25] Most calculations are carried out at the unrestricted Becke3LYP level,[26] with some test calculations being carried at the unrestricted Hartree–Fock (UHF) level. Several basis sets are applied. In all of them a quasi-relativistic effective core potential (ECP) replaces the 10 innermost electrons of Fe.[27] The basis set for Fe is always the valence double-ζ contraction labeled LANL2DZ associated to this ECP.[25, 27] In basis set I, used in all calculations unless otherwise stated, the basis set is 6-31G(d) for N, O;[28, 29] and STO-3G for C, H.[30] Five other basis sets are constructed through modifications in the description of

these atoms. Basis set II uses a STO-3G description for N, O, C, H.[30] Basis set III places 6-31G on N, O;[28] and STO-3G on C, H. In basis set IV, the 6-31G set is applied on N, O, C, H. Basis set V uses 6-31G(d) for N, O; and 6-31G for C, H. Finally, basis set VI consists of a 6-31G(d) description for N, O, C, H. Basis sets II to VI are only applied in the section devoted to evaluation of basis set quality. All geometry optimizations in the pure QM calculations are complete, with no symmetry restrictions. Spin contamination, measured through the expectation of S^2, was in all cases small.

IMOMM calculations were carried out with a program built from modified versions of the two standard programs Gaussian 92/DFT[31] and mm3(92).[32] The quantum mechanics region is defined by atoms with labels inferior to 15 in Scheme 1. Thus, the heme group is modeled in the quantum region as $[Fe(NH(CH)_3NH)_2]$, as in previous QM calculations,[23] and the imidazole as $NHCH_2$, with the dioxygen being introduced as such. The rest of the system constitutes the molecular mechanics region. The introduction of this QM/MM partition within the porphyrin ring has the inconvenient of downgrading the symmetry of the 4-coordinate system from D_{4h} to D_{2h}, but is in our opinion the best alternative. Other partitions with a smaller QM region could hardly keep the four equivalent sp^2 nitrogen atoms together with the dianionic nature of the porphyrin. The use of larger QM regions, apart from the associated increase in computational cost, is limited by the requirement of the IMOMM method, at least in its original formulation,[21] that no direct chemical bonds can be put between set 3 atoms, those connecting the QM and MM regions. This means that if, for instance, atoms C20 to C25 (Scheme 1) where introduced in the QM region, then the whole porphyrin, with atoms C26 to C31, would have to be included, because of the existence of bonds like that between C26 and C27. A final comment on the QM/MM partition concerns the imidazole ring. C15 and not C16 (Scheme 1) was included in the QM region because in the most simple Lewis structure of imidazole, the double bonds are between N14—C15 and C16—C18.

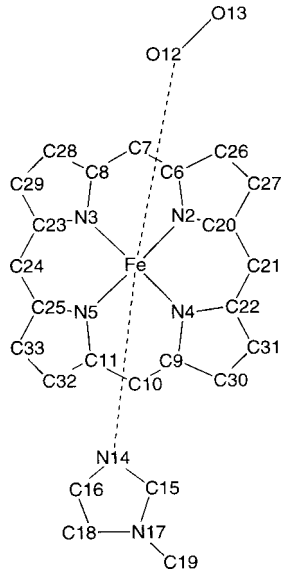

SCHEME 1.

The QM part of the IMOMM calculation uses the same methods and basis sets described above for the pure QM calculations. The MM calculations use the mm3(92) force field.[33] Van der Waals parameters for the iron atom are taken from the UFF force field,[34] and torsional contributions involving dihedral angles with the metal atom in terminal position are set to zero. MM stretching and bending terms involving Fe are set to zero by the IMOMM method in the current QM/MM partition, and because of that no MM parameters are required for them. All geometrical parameters are optimized except the bond distances between the QM and MM regions of the molecules. The frozen values are 1.019 Å (N—H), 1.101 Å (C—H) in the QM part; and 1.378 Å (N—C, porphyrin ring), 1.332 Å (C—C), 1.414 Å (N—C, imidazole ring) in the MM part.

Atom numbering is that shown in Scheme 1. The molecule is oriented in such a way that the porphyrin ring is in the *xy* plane, and the projections of the Fe—N bonds lie approximately on the bisectors of the *x* and *y* axis.

The 4-Coordinate [Fe(P)] System

The heme group as such has little direct application in biochemistry, but it is a natural starting point for both the experimental and the theoretical study. The crystal structures of a number of derivatives of heme have been reported, with different substituents in the ring. Unfortunately, the simplest model, with all substituents being hydrogen, has not been reported. Because of this, comparison will be made with a species containing some substituents. In particular, we have chosen [Fe(TPP)] (TPP = *meso*-tetraphenylporphyrin).[10] The electronic state of this particular molecule is well known experimentally to correspond to a triplet ($S = 1$). X-ray studies of electron distribution have even allowed the experimental assignment of the electronic state.[10] This assignment has also been

confirmed by recent theoretical studies.[35] In the ground state, the distribution of the electrons in the d orbitals of iron is the following: $d_{x^2-y^2}, d_{z^2}$, doubly occupied; d_{xz}, d_{yz}, singly occupied; d_{xy}, empty. Calculations are done only on this electronic state.

Calculations have been carried out on the [Fe(P)] model system at both the pure Becke3LYP and the IMOMM(Becke3LYP:MM3) computational levels. The optimized geometry from the IMOMM calculation is presented in Figure 1, and selected structural parameters of both calculations and experiment are collected in Table I. One first comment concerns the symmetry of the optimized geometry. Although all calculations were carried out without symmetry restrictions, the resulting geometries happen to have high symmetry. This is D_{4h} for the pure QM calculation and D_{2h} for the hybrid QM/MM calculation. Both computed geometries are planar (with an out of plane displacement of the atoms of 0°) and the difference in the symmetry of both geometries stems obviously from the partition in two different regions introduced in the IMOMM calculation. The contrast between the computed planar structures and the C_1, nearly S_4, symmetry of the experimental geometry was less expected. We attribute this difference to the fact that while the calculations are carried out on a gas phase [Fe(P)], experimental results are on a crystal structure of [Fe(TPP)]. The distortion from planarity in the experimental structure can be due to the presence of the phenyl groups,[36] or to packing effects.[37] Clarification of the origin of distortion from planarity in the experimental structure would require a further analysis, and is not the goal of this work.

Apart from the planarity, reflected in the average displacement out of the plane of the 24 atoms of the porphyrin ring, other data in Table I deserve comment. The agreement in bond angles between both computed geometries and the X-ray structure is excellent, with discrepancies always smaller than 2°. Discrepancies in bond distances are larger in a number of cases. Some of them were, nevertheless, to be expected. This is the case of the C20—C21, C20—C27, and C26—C27 distances. These distances have values of 1.395, 1.439, and 1.365 Å, respectively, in X-ray; 1.402, 1.459, and 1.367 Å, respectively, in Becke3LYP; and 1.336, 1.345, and 1.333 Å, respectively, in IMOMM. Agreement between experiment and pure QM is good (within 0.02 Å), while the discrepancy with IMOMM is up to 0.11 Å. An inspection of Scheme 1 shows that all these atoms are in the part purely described with the MM method, and the optimized IMOMM values are very close to the optimal bond distance for these types of atoms in the applied force field, which is 1.332 Å. A modification of the force field would undoubtedly correct this result. However, to keep the fairness of the test, introduction of experimental parameters in the calculation has been kept to a minimum.

TABLE I.
Selected Geometrical Parameters (Å and Degrees) from the Geometry Optimization of [Fe(P)] with the Pure Becke3LYP and with the IMOMM(Becke3LYP:MM3) Methods.

	Experiment	Pure QM	QM/MM
Fe—N2	1.966	2.016	1.940
N2—C6	1.378[a]	1.397	1.362
N2—C20	1.378[a]	1.397	1.378[b]
C6—C7	1.395[a]	1.402	1.401
C6—C26	1.439[a]	1.459	1.438[b]
C20—C21	1.395[a]	1.402	1.336
C20—C27	1.439[a]	1.459	1.345
C26—C27	1.365[a]	1.367	1.333
Fe—N2—C6	127.2[a]	127.4	128.7
Fe—N2—C20	127.2[a]	127.4	126.7
N2—Fe—N3	90.0[a]	90.0	89.5
N2—Fe—N4	90.0[a]	90.0	90.5
N2—C6—C7	125.3[a]	125.5	126.9
N2—C6—C26	110.6[a]	110.4	109.0
N2—C20—C21	125.3[a]	125.5	125.4
N2—C20—C27	110.6[a]	110.4	111.5
Fe-plane[c]	0.000	0.000	0.000
RMS displ.[d]	0.237	0.000	0.000

Experimental data on the [Fe(TPP)] system are also provided for comparison. Labeling of atoms is that from Scheme 1.
[a] Average values.
[b] Frozen in calculation.
[c] Distance of the iron atom to the mean plane of the porphyrin ring.
[d] Average out of plane displacement of the 24 atoms of the porphyrin ring.

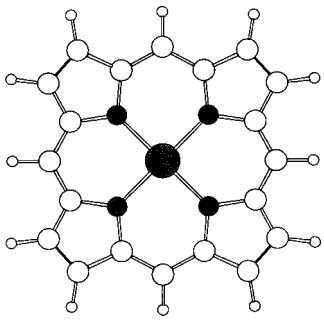

FIGURE 1. Optimized IMOMM(Becke3LYP:MM3) geometry of the 4-coordinate complex [Fe(P)].

Another discrepancy in the geometries appears in the Fe—N distance. This is more puzzling, because the distance oscillates between 2.016 Å for pure QM and 1.940 Å for the hybrid QM/MM, with the experimental value of 1.966 Å lying in between. Although the discrepancy of 0.05 Å with respect to the experimental number is in no case dramatic, this result could raise some concern on the accuracy of the description of the Fe—N bond in the IMOMM calculation. Furthermore, the overall agreement of the optimized geometries between them and with experiment could also be attributed to the steric constraints introduced by the presence of the porphyrin ring in the MM part of the calculation. In other words, one could still argue that the QM properties of the region around the metal atom are not well reproduced. Because of this, a more exigent test than comparison of optimized geometries was carried out.

The energy cost of the out of plane displacement of the metal atom was examined through both pure Becke3LYP and IMOMM(Becke3LYP:MM3) calculations. The iron atom was displaced within the symmetry axis of the system, keeping the rest of the geometry frozen at the respective optimized values. The energy cost of this type of movement will be ruled almost exclusively by electronic effects, i.e., by the binding of the Fe to the N atoms of the porphyrin ring. It will be, therefore, a good test of the quality of the description of this binding. Furthermore, it has a chemical interest in itself, because this type of movement of the metal atom seems to be a key factor in the behavior of a number of biological heme groups. The energy cost of the out of plane displacement of Fe in the 4-coordinate system computed with the two different methods is presented in Figure 2. The agreement between the two computational levels is excellent. The discrepancy between both calculations is always inferior to 1 kcal/mol, even with displacements as large as 0.5 Å, with a high energy cost of ca. 20 kcal/mol. It follows that the description of the Fe—N bond is essentially the same in both calculations, regardless of the fact that only part of the aromatic ring is treated quantum mechanically in the IMOMM calculation.

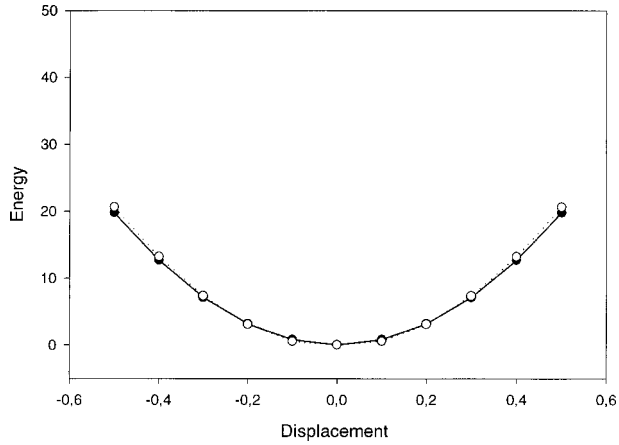

FIGURE 2. Energy cost (in kcal/mol) associated to the out-of-plane displacement (in Å) of the Fe atom in the 4-coordinate system. Solid line and solid circles correspond to the pure QM calculation, and dashed line and empty circles correspond to the hybrid QM/MM calculation.

The 5-Coordinate [Fe(P)(Im)] System

Coordination of an imidazole ligand to the heme group leads to a 5-coordinate species with a square pyramidal geometry. This type of compounds are good biomimetic models of deoxymyoglobin and deoxyhemoglobin, the imidazole replacing the proximal histidine of the biological systems. The need to avoid both the dimerization and the formation of the 6-coordinate species with the two axial ligands poses serious restrictions on the nature of the porphyrins able to give this kind of complexes. For our comparison, we have chosen the species [Fe(Piv_2C_8)(1 − (Me)Im)] (Piv_2C_8 = α,α,5,15-[2,2′-(octanediamido)diphenyl]-α,α,10,20-bis(*o*-pivalamidophenyl)porphyrin) among the available structures.[38] This species has the advantage for our comparison of having 1-methylimidazole as axial ligand, in contrast with the more common 2-methylimidazole, which is more sterically demanding.

Unfortunately, neither for [Fe(Piv_2C_8)(1 − (Me) Im)] nor for other 5-coordinate derivatives of heme the electronic state is experimentally known. Electronic spectroscopy, magnetic susceptibility and Mössbauer measurements are conclusive in identifying it as high spin ($S = 2$, with four unpaired electrons on the iron atom), but are unable to find the molecular orbitals where the unpaired electrons are. This question is not trivial. The iron atom, formally Fe(II), has six valence electrons, to be placed in its *d* orbitals. The high-spin state means that four of the orbitals are singly occupied, and the remaining one is doubly occupied. Even after discarding the clearly antibonding d_{xy} and d_{z^2} orbitals, there are still three good candidates to be the doubly occupied orbital. These are $d_{x^2-y^2}$, d_{xz}, and d_{yz}, all of them nonbonding in the absence of π interactions.

Full *ab initio* geometry optimizations have been carried out on the [Fe(P)(NH=CH_2)] complex with the three different electronic states emerging from the double occupancy of each of these three atomic orbitals. The ground state happens to have two electrons in a linear combination of d_{xz} and d_{yz}, followed 1.8 kcal/mol above by the state with the other linear combination of these same orbitals doubly occupied. The excited state with the $d_{x^2-y^2}$ orbital doubly occupied has a higher relative energy of 2.2 kcal/mol. The close relationship between d_{xz} and d_{yz} could be expected *a priori*, because the equivalence between them is only broken by the π effects of the imidazole ligand. At any rate, our calculations predict that the valence β electron of iron will be placed in these axial orbitals, and not in the equatorial $d_{x^2-y^2}$ orbital.

Calculations were carried out on the ground state at the Becke3LYP and IMOMM(Becke3LYP:MM3) computational levels. The pure QM calculations were performed on the [Fe(P)(NH=CH_2)] model system, where the imine ligand tries to reproduce the electronic effects of imidazole. The hybrid QM/MM calculations were carried out on the [Fe(P)(1−(Me)Im)] system. Selected geometrical parameters are collected in Table II. The optimized IMOMM structure is presented in Figure 3. Internal bond lengths and bond angles within the porphyrin ring follow exactly the same trends discussed above for 4-coordinate complexes, and are therefore not presented. It is, however, worth mentioning the RMS deviation from planarity of the 24 atoms of the porphyrin ring. The computed values at both the pure QM and the QM/MM levels are near 0.05 Å, in sharp contrast with the value of 0.00 Å obtained in the 4-coordinate system. Though the computed values are still far from the experimental value of 0.131 Å, this discrepancy is likely related to the presence of the large substituents in the porphyrin. Our calculations confirm at any rate that there is an intrinsic deviation from planarity associated to the coordination of a fifth ligand. The observed distortion points toward a C_{4v} arrangement.

The average distances between the metal atom and the nitrogen atoms in the porphyrin ring show the same type of dispersion already observed in the 4-coordinate complex, with the experimental value lying between the pure Becke3LYP and IMOMM(Becke3LYP:MM3) values. All the Fe—N_p distances in this 5-coordinate complex are longer by ca. 0.1 Å than those in their 4-coordinate counterpart. This is fully consistent with the shift from low spin to high spin in the metal involving the placement of one electron in the antibonding d_{xy} orbital.

TABLE II.
Selected Geometrical Parameters (Å and Degrees) from the Geometry Optimization of [Fe(P)(NH=CH_2)] with the Pure Becke3LYP and of [Fe(P)(1 − (Me)Im)] with the IMOMM(Becke3LYP:MM3) Methods.

	Experiment	Pure QM	QM/MM
Fe—N_p[a]	2.074	2.101	2.029
Fe—N14	2.134	2.252	2.233
N14—C15	1.35	1.279	1.299
N14—C16	1.25	—[b]	1.414[c]
Fe—N14—C15	127.	126.1	136.8
Fe—N14—C16	120.	120.6	122.6
N2—Fe—N14—C15	−54.	−90.0	−43.2
Fe-plane[c]	−0.342	−0.316	−0.411
RMS displ.[d]	0.131	0.043	0.054

Experimental data on the [Fe(Piv_2C_8)(1 − (Me)Im)] system are also provided for comparison. Labeling of atoms is that from Scheme 1.
[a] Average values.
[b] Corresponds to N—H in this calculation.
[b] Frozen in calculation.
[c] Distance of the iron atom to the mean plane of the porphyrin ring.
[d] Average out of plane displacement of the 24 atoms of the porphyrin ring.

Most data in Table II focus on the description of the imidazole ligand. The Fe—N_{im} distance is longer by ca. 0.10 Å in calculation than in experiment. We are not able to explain the origin of this discrepancy. At any rate, both computed values are very close to each other (2.252 Å vs. 2.233 Å), proving that the use of the QM/MM method does not introduce any error. Overall agreement in the geometrical parameters is correct. Moreover, one has to take with some suspicion the X-ray parameters of the imidazole ligand, which would make the N=C double

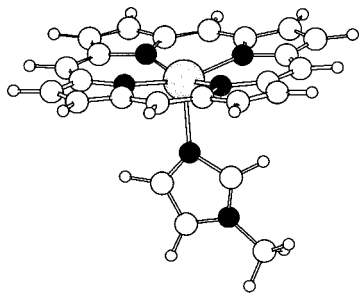

FIGURE 3. Optimized IMOMM(Becke3LYP:MM3) geometry of the 5-coordinate complex [Fe(P)(1 − (Me)Im)].

bond N14—C15 of imidazole longer than the N—C single bond N14—C16.

The sharper discrepancy shown in Table II concerns the N2—Fe—N14—C15 dihedral angle. This angle measures the rotation around the Fe—N14 single bond, and rules the placement of the imidazole plane with respect to the porphyrin ring. Its sign is arbitrary, because the x and y directions are equivalent in absence of axial ligand. We have chosen a negative sign for consistence with data on the 6-coordinate complex presented below. An angle of -90.0 degrees (like in the pure QM calculation) means that the imidazole plane is eclipsing one of the Fe—N_p bonds, while an angle of -45.0 degrees (close to the $-43.2°$ found in the QM/MM calculation) indicates a staggered orientation of the imidazole with respect to the Fe—N_p bonds. The two computed values are, therefore, just opposite, with the experimental value ($-54°$) lying in between, although closer to the QM/MM value. The importance of this large discrepancy between different values is, however, arguable, because there is also a large dispersion in different experimental 5-coordinate derivatives of heme,[8] as well as in experimental reports of deoxymyoglobin and deoxyhemoglobin. It seems, therefore, that rotation around this single bond has a very low barrier. We are planning to further analyze this question, but preliminary calculations confirm a very low barrier of 1.5 kcal/mol in pure QM calculations on [Fe(P)(Im)].

A final number to mention from Table II is the displacement of the iron atom out of the 24-atom porphyrin plane. This is one of the most important parameters, because it seems to play a critical role in the cooperativity of hemoglobin involved in the allosteric transition. In this case, agreement between experiment and calculation is good, with values of -0.342, -0.316, and -0.411 Å, for the experiment and the two calculations, respectively. The negative value corresponds to the fact that the displacement is towards the imidazole, and away from the empty site.

The energy cost of the out-of-plane displacement of the metal atom was also examined in the 5-coordinate system. In this case, the displacement was carried out in the direction of the Fe—N_{im} bond. Moreover, the axial ligand was moved together with the metal, with the Fe—N_{im} distance being frozen at the corresponding optimized value. The results are shown in Figure 4. Again, agreement is very good, with the curves computed through pure QM and through hybrid QM/MM methods lying very close to each other. It is worth mentioning also that the out-of-place displacement is less energy demanding in the 5-coordinate system (ca. 5 kcal/mol for a move of 0.3 Å) than it was for the 4-coordinate system (ca. 10 kcal/mol for the same move of 0.3 Å). This difference between the two systems is well reproduced in the IMOMM calculation.

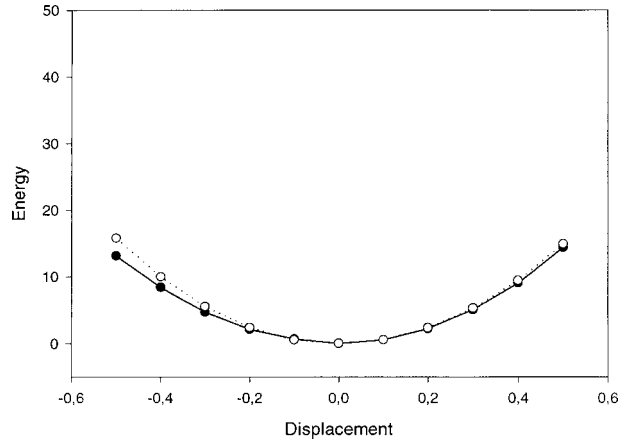

FIGURE 4. Energy cost (in kcal/mol) associated to the out-of-plane displacement (in Å) of the Fe atom around its equilibrium position in the 5-coordinate system. Solid line and solid circles correspond to the pure QM calculation, and dashed line and empty circles correspond to the hybrid QM/MM calculation.

An additional result that can be obtained from the calculations presented in this section and the previous one is an estimation of the binding energy of the axial imidazole ligand to the 4-coordinate complex. This can be done by direct substraction of the energy of the separated 4-coordinate plus imidazole fragments from that of the 5-coordinate. The result of this operation presents a rather poor agreement between the two calculations, with values of -2.7 kcal/mol for the pure QM calculation and $+8.4$ kcal/mol for the QM/MM calculation. These numbers should not be taken as direct estimations of the binding energy. Other, more ellaborate, schemes than this simple substraction have been suggested to compute binding energies in this type of systems,[15] and a number of possibly significant corrections, like basis set superposition error, have been neglected. However, the systematic errors should be the same in both calculations, and one would expect a more similar result. Our conclusion is that the hybrid QM/MM method applied, while performing well in predicting the equilibrium geometry and relative distortion energies from it, has a poorer performance in predicting the binding energy of the imidazole ligand.

Finally, a supplementary set of pure QM calculations on the 5-coordinate systems was carried out on [Fe(P)(Im)] and [Fe(P)(1 − (Me)Im)] to check for possible inaccuracies associated with the use of the [Fe(P)(NH=CH_2] model system. The optimized structures with the imidazole and methylimidazole ligands were found to be similar to those with the imine model. Discrepancies in bond distances within the Fe(P) unit were always smaller than 0.01 Å. The coordination of the axial ligand was, logically, more affected, but changes were also small. The Fe—N14 distance (2.252 Å) was 2.226 Å with imidazole, and 2.213 Å with methylimidazole. The out-of-plane displacement was also affected, with values of −0.363 Å for imidazole and −0.376 Å for methylimidazole (to be compared with −0.316 Å for the imine model). These small changes bring actually the QM results closer to the QM/MM ones (Table II), and do not explain in any case the discrepancies with the X-ray structures.

The 6-Coordinate [Fe(P)(Im)(O_2)] System

Coordination of a dioxygen molecule to the 5-coordinate species derivated from heme discussed in the previous section leads to 6-coordinate species with an octahedral geometry. These types of compounds are the biomimetic forms of oxymyoglobin and oxyhemoglobin. Despite their large interest, X-ray data have been reported only on two complexes with this stoichiometry: [Fe(T_{piv}PP)(1 − (Me)Im)(O_2)],[39] and [Fe(T_{piv}PP)(2 − (Me)Im)(O_2)].[40] Both complexes are quite similar, sharing the same porphyrin T_{piv}PP, which is *meso*-tetrakis($\alpha,\alpha,\alpha,\alpha$-*o*-pivalamidophenyl)porphyrin. We have chosen for comparison the [Fe(T_{piv}PP)(1 − (Me)Im)(O_2)] complex, containing the less sterically demanding 1-methylimidazole ligand.

A preliminary study[24] on the geometry optimization of this compound with the IMOMM (Becke3LYP:MM3) method has already been published, albeit with a slightly different basis set in the QM part. The change in the basis set introduces only minor modifications in the geometry, and the results are only briefly discussed here for completion of the methodological analysis. The spin state of this system has a singlet nature, and we have assumed in our calculations, as the authors of other theoretical studies,[23] that the three doubly occupied d orbitals of Fe are those corresponding to the t_{2g} set, namely $d_{x^2-y^2}$, d_{xz}, and d_{yz}. This is actually the electronic structure closest to the ground state obtained in CASSCF calculations with a large active space.

Recent DFT calculations by the group of Parrinello[16] indicate that the ground state of this system is an open-shell singlet, where one electron of one of the two doubly occupied d_π orbitals of Fe is transferred to the π^* orbital of O_2, resulting in a Fe^{III}—O_2^- system. Our attempts to reproduce this result, obtained with a plane wave algorithm,[16] with the more conventional algorithms of the Gaussian program[25] through the use of a spin-contaminated broken symmetry solutions have lead to structures where the dioxygen unit dissociates from the metal center. We attribute the discrepancy in results to the difference in the computational method. We are aware of the potential relevance of this controversy to the chemistry of the system. However, because the difference between the open-shell and close-singlets is concentrated in the Fe—O_2 subunit, within the QM region, we consider it does not affect the validity of the introduction of a QM/MM partition within the porphyrin ring, which is the subject of this article.

Calculations were carried out on the closed-shell singlet electronic state at the Becke3LYP and IMOMM(Becke3LYP:MM3) computational levels. The pure QM calculations were performed on the [Fe(P)(NH=CH_2)(O_2)] system, and hybrid QM/MM calculations were carried out on the [Fe(P)(1−(Me)Im)(O_2)] system. Selected geometrical parameters are collected in Table III, and the optimized IMOMM structure is presented in Figure 5. A number of the results of the geometry optimization confirm trends already observed on the calculations on the other two systems. Internal geometrical parameters of the porphyrin ring are practically the same, and are not included because of the little changes with respect from those of the 4-coordinate and 5-coordinate system. The computed RMS deviation of the 24 atoms of the porphyrin ring from the plane is of the same order than that of the 5-coordinate system. The experimental Fe—N_p distance is again shorter than that obtained in the QM calculation and longer than that obtained in the QM/MM calculation. The experimental trend of having this Fe—N_p distance in the 6-coordinate system slightly longer than in the 4-coordinate system and quite shorter than in the 5-coordinate system is, nevertheless, well reproduced by both levels of calculation. A description of the coordination of imidazole presents similar problems to those already observed in the 5-coordinate system. The shortening of the Fe—N14 distance associated to the loss of one α electron from the antibonding d_{z^2} orbital is, nevertheless,

TABLE III.
Selected Geometrical Parameters (Å and Degrees) from the Geometry Optimization of [Fe(P)(NH=CH$_2$)(O$_2$)] with the Pure Becke3LYP and of [Fe(P)(1 − (Me)Im)(O$_2$)] with the IMOMM(Becke3LYP:MM3) Methods.

	Experiment	Pure QM	QM/MM
Fe—N$_p$[a]	1.978	2.035	1.949
Fe—N14	2.070	2.050	2.167
Fe—O12	1.746	1.757	1.759
O12—O13	1.163	1.268	1.286
Fe—O12—O13	129.4	121.1	117.0
O12—Fe—N14	180.0	175.8	179.4
N2—Fe—N14—C15	159.5	177.9	133.0
N2—Fe—O12—O13	−42.4	−44.6	−45.9
Fe-plane[b]	+0.014	+0.019	+0.061
RMS displ.[c]	0.072	0.044	0.033

Experimental data on the [Fe(T$_{piv}$PP)(1 − (Me)Im)(O$_2$)] system are also provided for comparison. Labeling of atoms is that from Scheme 1.
[a] Average values.
[b] Distance of the iron atom to the mean plane of the porphyrin ring.
[c] Average out of plane displacement of the 24 atoms of the porphyrin ring.

well reproduced in the calculation. The values for the dihedral angle ruling the rotation around the Fe—N14 bond are also very different. In this case, the best agreement with experiment is given by the pure QM calculation.

Parameters concerning the coordination of O_2 and the out of plane displacement of Fe, which are probably the most critical for the biochemical activity of hemoglobin, are very well reproduced. The two computed values for the Fe—O distance, 1.757 and 1.759 Å, are practically identical to the experimental value of 1.746 Å. The two computed values (1.268, 1.286 Å) for the O—O distance are close to each other, but far from the experimental report of 1.163 Å. However, the experimental value (even shorter than the value of 1.21 Å for free oxygen!) is suspect, because of the disorder on the placement of the second oxygen within the crystal, as admitted by the authors of the X-ray experiment themselves.[39] A similar reasoning can be used for the Fe—O—O bond angles, which are, nevertheless, in all cases indicative of a bent η^1 coordination mode, where only one of the oxygen atoms is directly attached to the metal. The orientation of the Fe—O—O plane with respect to the Fe—N$_p$ axis is staggered, in both calculations (−44.6°, −45.9°) and in the experiment (−42.4°). Finally, the iron atom is computed to lie in the energy minimum very close to the porphyrin plane, with a deviation smaller than 0.1 Å, always towards the oxygen. This is, again, in agreement with the experiment, and very different from the behavior of the 5-coordinate system.

To finish the study on the 6-coordinate systems, the energy cost of the out-of-plane displacement of the metal atom was also studied. In this case, the iron atom was displaced also along the Fe—N$_{im}$ direction, and it was moved together with the two axial ligands. The results are presented in Figure 6. Although agreement is not as perfect as in the other two cases previously analyzed, the overall similarity between the Becke3LYP and the IMOMM(Becke3LYP:MM3) curves is still remarkable. The out-of-plane displacement is more energetically costly in this case of the 6-coordinate

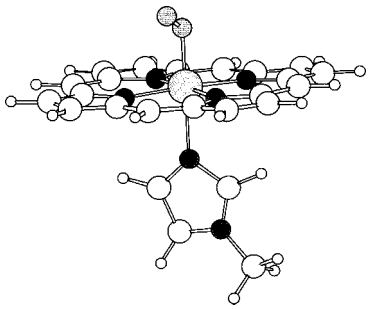

FIGURE 5. Optimized IMOMM(Becke3LYP:MM3) geometry of the 6-coordinate complex [Fe(P)(1 − (Me)Im)(O$_2$)].

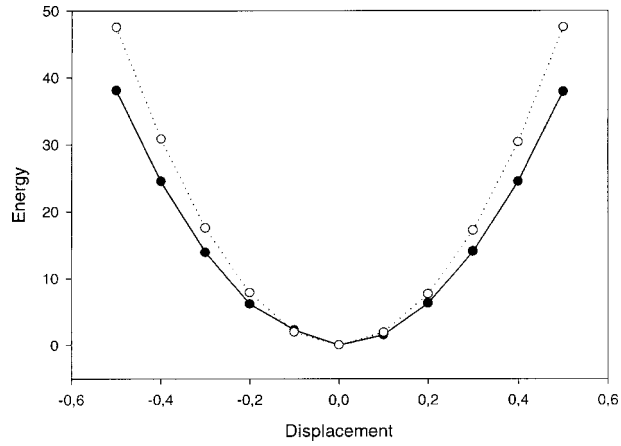

FIGURE 6. Energy cost (in kcal/mol) associated to the out-of-plane displacement (in Å) of the Fe atom around its position of equilibrium in the 6-coordinate system. Solid line and solid circles correspond to the pure QM calculation, and dashed line and empty circles correspond to the hybrid QM/MM calculation.

species, with an increase of ca. 15 kcal/mol for a move of 0.3 Å. This behavior, which may have interesting implications on the reactivity of the system, is well reproduced in the cheaper hybrid calculation.

Finally, the binding energy of dioxygen to the 5-coordinate system was evaluated through substraction of the energy of the separated fragments from that of the 6-coordinate system. The resulting values were +9.5 and +5.6 kcal/mol for the pure QM and the QM/MM calculations, respectively. Although agreement is better than for the binding energy of imidazole, this magnitude remains by far the worst reproduced by the QM/MM calculation among those considered.

QM Calculations on Small Model Systems

Results in the previous sections prove that the IMOMM calculations provide results of comparable quality to those of much more expensive pure QM calculations. In fact, the cost of the IMOMM calculation is equivalent to that of a pure QM calculation on the QM region of the hybrid calculation, because the computational cost of the MM part is in practice neglectable. It is, therefore, interesting to evaluate the quality of a pure QM calculation on the model system used for the QM region of the IMOMM calculation. If the result were not different from that of the IMOMM calculation, the introduction of the MM region would be useless.

A pure QM calculation was carried out on the $[Fe(NH(CH)_3NH)_2(Im)]$ system. Although some parameters (namely, the Fe—N distances) were similar to those obtained in the IMOMM calculations on the 5-coordinate systems, very substantial differences appeared in two parameters. These were the out-of-plane displacement of the metal atom and the RMS displacement of atoms in the porphyrin ring. The out-of-plane displacement of Fe, which has values around 0.3–0.4 Å for [Fe(P)(Im)] systems (Table II), climbs to a value of 0.652 Å in this pure QM calculation on the model system. The RMS displacement increases even more substantially, from values below 0.1 Å for [Fe(P)(Im)] to a value of 0.331 Å in $[Fe(NH(CH)_3NH)_2(Im)]$. The qualitative difference between those distances is certainly in the loss of planarity of the remains of the porphyrin ring in the pure QM calculation. In this new calculation they rearrange themselves in two different planes, one for each fragment, with no correlation between them. The distortions from planarity, which have been postulated as important factors in the biological properties of heme groups,[36, 41, 42] will, therefore, be poorly reproduced by pure QM calculations on small model systems.

Methodological Discussion on the QM Calculations

The quantum mechanics part absorbs most of the computer effort of the IMOMM calculation. Moreover, available QM methods come at very different computational prices, the most expensive usually providing the highest quality. It is, therefore, important to choose the cheapest QM method able to provide the desired quality. This section contains a brief discussion on the reasons justifying the choice of the QM methods applied in the rest of the work. In particular, basis sets of different qualities are tested; and the unrestricted Becke3LYP method is confronted with the cheaper unrestricted Hartree–Fock method.

Tables IV and V present the results of the application of different basis sets to the calculation of the 4-coordinate system at the IMOMM(UHF:MM3) and IMOMM(Becke3LYP:MM3) levels. Basis sets II to VI, defined in the computational details, are numbered by order of increasing quality. Basis set I, the one used in the rest of the article, would involve a similar computational effort to that of basis set IV. Tables IV and V show that the basis set has little effect on the parameters under discussion. The most sensitive geometrical parameter is the Fe—N2 distance with a dispersion of 0.039 Å at the IMOMM(UHF:MM3) level, and of 0.029 Å at the IMOMM(Becke3LYP:MM3) level. Nevertheless, most of this dispersion is related to the presence of the smaller basis set II, minimal for all atoms but the metal. If this basis set II is taken out, the dispersion in Fe—N2 distances comes down to 0.007 and 0.005 Å, respectively. That is, all the five better basis sets yield results identical to the 1/10 of an Å. The energy cost for the out of plane displacement of iron seems to be a little more sensitive to the basis set, albeit exaggerated because of the large displacement of 0.5 Å being considered. Again, basis set II stands out from the rest, and can be directly discarded. The other five basis sets can be divided in this case in two groups. Basis sets III and IV are very close to each other (dispersions of 0.4 and 0.1 kcal/mol, at the UHF and UBecke3LYP levels); and more distanced from I, V, and VI, which are also grouped together (dispersions of 0.2 at both computational levels). The key factor seems to be the basis set at

TABLE IV.
Selected Results (Å, Degrees, and kcal/mol) from the IMOMM(UHF:MM3) Geometry Optimization of the 4-Coordinate [Fe(P)] with Different Basis Sets.

	I	II	III	IV	V	VI
Fe—N2	1.981	1.947	1.979	1.986	1.986	1.982
N2—C6	1.341	1.348	1.344	1.329	1.321	1.316
C6—C7	1.387	1.386	1.384	1.389	1.393	1.392
Fe—N2—C6	127.6	127.9	127.6	127.5	127.4	127.5
Fe—N2—C20	125.8	126.8	125.4	125.3	125.7	125.5
N2—Fe—N3	89.2	89.6	89.0	88.9	89.2	89.0
N2—Fe—N4	90.8	90.4	91.0	91.0	90.8	91.0
Energy cost	16.3	22.9	18.7	19.1	16.5	16.4

The energy cost presented corresponds to the displacement of the Fe atom 0.5 Å out of the plane of the molecule. Labeling of atoms is that from Scheme 1, and basis sets are defined in the Computational Details.

nitrogen, which is 6-31G for III, IV; and 6-31G(d) for I, V, and VI. The basis set at carbon and hydrogen, further away from the metal, has a much smaller effect. Because of this, we chose for the rest of the calculations basis set I, which is the cheapest one in the group providing the most accurate results.

Comparison between Tables IV and V shows that the results are more affected by the change of the method from UHF to UBecke3LYP than they are by the change of basis set within one method. Nevertheless, they are still quite similar. One could, therefore, be tempted to choose the cheaper UHF method for the QM part of all calculations. We certainly tried this strategy, with the result of an extremely poor description of the 6-coordinate system. What happens in the UHF calculation on [Fe(P)($NHCH_2$)(O_2)] is that the Fe—O oxygen distance increases to values above 3 Å (to be compared with the experimental or Becke3LYP value of ca. 1.75 Å). This means that the oxygen molecule does not bind to the complex at the UHF level. This failure is very probably related to the fact that this bond has an important component of backdonation from the metal center to the dioxygen unit, and backdonation is largely underestimated in the absence of electron correlation. It is worth mentioning that UHF calculations with a minimal basis set for oxygen provide a "pseudobonding" distance of ca. 2.2 Å. We relate this result to the basis set superposition error associated to the unbalance between the basis sets on the metal and on the oxygen. At any rate, the complete failure of the UHF method in the description of the 6-coordinate systems prompted us to discard it, and to use UBecke3LYP as the computational method throughout the article.

TABLE V.
Selected Results (Å, Degrees, and kcal/mol) from the IMOMM(Becke3LYP:MM3) Geometry Optimization of the 4-Coordinate [Fe(P)] with Different Basis Sets.

	I	II	III	IV	V	VI
Fe—N2	1.940	1.916	1.944	1.945	1.944	1.945
N2—C6	1.362	1.386	1.366	1.355	1.348	1.348
C6—C7	1.401	1.401	1.399	1.391	1.393	1.393
Fe—N2—C6	128.7	129.0	128.5	128.0	128.0	127.9
Fe—N2—C20	126.7	127.6	126.5	126.7	126.4	127.0
N2—Fe—N3	89.5	89.8	89.5	89.7	89.8	89.9
N2—Fe—N4	90.5	90.2	90.5	90.3	90.2	90.1
Energy cost	19.8	23.5	21.3	21.4	20.0	19.9

The energy cost presented corresponds to the displacement of the Fe atom 0.5 Å out of the plane of the molecule. Labeling of atoms is that from Scheme 1, and basis sets are defined in the Computational Details.

Concluding Remarks

IMOMM(Becke3LYP:MM3) calculations on the 4-coordinate [Fe(P)], the 5-coordinate [Fe(P)(1 − (Me)Im)], and the 6-coordinate [Fe(P)(1 − (Me)Im)(O_2)] systems give results that are in good agreement with full QM calculations on analogous systems. Agreement is especially close in the case of optimized geometrical parameters and the energy cost of displacement of the iron atom out of the plane of the porphyrin ring. Discrepancies are more significant in the case of the binding energy of the axial ligands to the heme group. Optimized geometries are also close to experimental X-ray geometries, and the differences are likely associated to the experimental existence of bulky substituents in the porphyrin and of crystal packing effects, which are absent from the gas phase calculations.

The use of an MM description for a significant part of the heme group porphyrin ring, therefore, brings a major reduction in computer effort with a minor reduction of quality in the results—very minor in some properties. The application of hybrid QM/MM methods to systems containing heme groups thus appears as a very promising venue for the theoretical study of the structure and reactivity of these biologically relevant systems.

Acknowledgment

J.-D.M. thanks the computational support from the IDRIS Supercomputer Center of the CNRS (France).

References

1. (a) Perutz, M. F. Proc R Soc Lond Ser B 1980, 208, 135; (b) Perutz, M. F.; Fermi, G.; Luisi, B.; Shaanan, B.; Liddington, R. C. Acc Chem Res 1987, 20, 309.
2. Welinder, K. G. Curr Opin Struct Biol 1992, 2, 388.
3. Malmström, B. G. Chem Rev 1990, 90, 1247.
4. Sono, M.; Roach, M. P.; Coulter, E. D.; Dawson, J. H. Chem Rev 1996, 96, 2841.
5. Barber, J.; Andersson, B. Nature 1994, 370, 31.
6. Dremma, C. L. S.; Huang, J. T.; Drummond, R. G.; Matthews, R. G.; Ludwig, M. L. Science 1994, 266, 1669.
7. Halcrow, M. A.; Christou, G. Chem Rev 1994, 94, 2421.
8. Momenteau, M.; Reed, C. A. Chem Rev 1994, 94, 659.
9. (a) Dedieu, A.; Rohmer, M.-M.; Veillard, A. Adv Quantum Chem 1982, 16, 43; (b) Rohmer, M.-M.; Dedieu, A.; Veillard, A. Chem Phys 1983, 77, 449; (c) Rohmer, M.-M. Chem Phys Lett 1985, 116, 44.
10. Li, N. Y.; Su, Z. W.; Coppens, P.; Landrum, J. J Am Chem Soc 1990, 112, 7294.
11. (a) Spiro, T. G.; Kozlowski, P. M. J Biol Inorg Chem 1997, 2, 516; (b) Spiro, T. G.; Kozlowski, P. M. J Am Chem Soc 1998, 120, 4524.
12. Vangberg, T.; Bocian, D. F.; Ghosh, A. J Biol Inorg Chem 1997, 2, 526.
13. (a) Jewsbury, P.; Yamamoto, S.; Minato, T.; Saito, M.; Kitagawa, T. J Am Chem Soc 1994, 116, 11586; (b) Jewsbury, P.; Yamamoto, S.; Minato, T.; Saito, M.; Kitagawa, T. J Phys Chem 1995, 99, 12677.
14. Ghosh, A.; Bocian, D. F.; J Phys Chem 1996, 100, 6363.
15. Sigfridsson, E.; Ryde, U. J. Biol Inorg Chem 1999, 4, 99.
16. (a) Rovira, C.; Ballone, P.; Parrinello, M. Chem Phys Lett 1997, 271, 247; (b) Rovira, C.; Kunc, K.; Hutter, J.; Ballone, P.; Parrinello, M. J Phys Chem 1997, 101, 8914; (c) Rovira, C.; Kunc, K.; Hutter, J.; Ballone, P.; Parrinello, M. Int J Quant Chem 1998, 69, 31; (d) Rovira, C.; Parrinello, M. Chem Eur J 1999, 5, 250; (e) Rovira, C.; Carloni, P.; Parrinello, M. J Phys Chem B 1999, 103, 7031.
17. (a) Salzmann, R.; McMahon, M. T.; Godbout, N.; Sanders, L. K.; Wojdelski, M.; Oldfield, E. J Am Chem Soc 1999, 121, 3818; (b) Godbout, N.; Sanders, L. K.; Salzmann, R.; Havlin, R. H.; Wojdelski, M.; Oldfield, E. J Am Chem Soc 1999, 121, 3829.
18. (a) Loew, G.; Dupuis, M. J Am Chem Soc 1996, 118, 10584; (b) Harris, D. L.; Loew, G. H. J Am Chem Soc 1996, 118, 10588; (c) Harris, D.; Loew, G.; Waskell, L. J Am Chem Soc 1998, 120, 4308; (d) Woon, D. E.; Loew, G. H. J Phys Chem A 1998, 102, 10380.
19. Zakharieva, O.; Grodzicki, M.; Trautwein, A. X.; Veeger, C.; Rietgens, I. M. C. M. J Bioinorg Chem 1996, 1, 192.
20. Green, M. T. J Am Chem Soc 1998, 120, 10772.
21. Maseras, F.; Morokuma, K. J Comput Chem 1995, 16, 1170.
22. (a) Matsubara, T.; Maseras, F.; Koga, N.; Morokuma, K. J Phys Chem 1996, 100, 2573; (b) Barea, G.; Maseras, F.; Jean, Y.; Lledós, A. Inorg Chem 1996, 35, 6401. (c) Maseras, F.; Eisenstein, O. New J Chem 1998, 22, 5; (d) Ujaque, G.; Cooper, A. C.; Maseras, F.; Eisenstein, O.; Caulton, K. G. J Am Chem Soc 1998, 120, 361; (e) Cooper, A. C.; Clot, E.; Huffman, J. C.; Streib, W. E.; Maseras, F.; Eisenstein, O.; Caulton, K. G. J Am Chem Soc 1999, 121, 97; (f) Ujaque, G.; Maseras, F.; Lledós, A. J Am Chem Soc 1999, 121, 1317.
23. Bytheway, I.; Hall, M. B. Chem Rev 1994, 94, 639.
24. Maseras, F. New J Chem 1998, 22, 327.
25. Frisch, M. J.; Trucks, G. W.; Schlegel, H. B.; Gill, P. M. W.; Johnson, B. G.; Robb, M. A.; Cheeseman, J. R.; Keith, T.; Petersson, G. A.; Montgomery, J. A.; Raghavachari, K.; Al-Laham, M. A.; Zakrzewski, V. G.; Ortiz, J. V.; Foresman, J. B.; Peng, C. Y.; Ayala, P. Y.; Chen, W.; Wong, M. W.; Andres, J. L.; Replogle, E. S.; Gomperts, R.; Martin, R. L.; Fox, D. J.; Binkley, J. S.; Defrees, D. J.; Baker, J.; Stewart, J. P.; Head-Gordon, M.; Gonzalez, C.; Pople, J. A. Gaussian 94; Gaussian, Inc., Pittsburgh, PA, 1995.
26. (a) Becke, A. D. J Chem Phys 1993, 98, 5648; (b) Lee, C.; Yang, W.; Parr, R. G. Phys Rev B 1988, 37, 785; (c) Stephens, P. J.; Devlin, F. J.; Chabalowski, C. F.; Frisch, M. J. J Phys Chem 1994, 98, 11623.
27. (a) Hay, P. J.; Wadt, W. R. J Chem Phys 1985, 82, 299.
28. Hehre, W. J.; Ditchfield, R.; Pople, J. A. J Chem Phys 1972, 56, 2257.

29. Hariharan, P. C.; Pople, J. A. Theor Chim Acta 1973, 28, 213.
30. Hehre, W. J.; Stewart, R. F.; Pople, J. A. J Chem Phys 1969, 51, 2657–2667.
31. Frisch, M. J.; Trucks, G. W.; Schlegel, H. B.; Gill, P. M. W.; Johnson, B. G.; Wong, M. W.; Foresman, J. B.; Robb, M. A.; Head-Gordon, M.; Replogle, E. S.; Gomperts, R.; Andres, J. L.; Raghavachari, K.; Binkley, J. S.; Gonzalez, C.; Martin, R. L.; Fox, D. J.; Defrees, D. J.; Baker, J.; Stewart, J. J. P.; Pople, J. A. Gaussian 92/DFT; Gaussian, Inc., Pittsburgh, PA, 1993.
32. Allinger N. L. mm3(92); QCPE: Bloomington IN, 1992.
33. (a) Allinger, N. L.; Yuh, Y. H.; Lii, J. H. J Am Chem Soc 1989, 111, 8551; (b) Lii, J. H.; Allinger, N. L. J Am Chem Soc 1989, 111, 8566; (c) Lii, J. H.; Allinger, N. L. J Am Chem Soc 1989, 111, 8576.
34. Rappé, A. K.; Casewit, C. J.; Colwell, K. S.; Goddard, W. A., III; Skiff, W. M. J Am Chem Soc 1992, 114, 10024.
35. Kozlowski, P. M.; Spiro, T. G.; Berces, A.; Zgierski, M. Z. J Phys Chem B 1998, 102, 2603.
36. Nakamura, M.; Ikeue, T.; Fujii, H.; Yoshimura, T. J Am Chem Soc 1997, 119, 6284.
37. Vangberg, T.; Ghosh, A. J Am Chem Soc 1998, 120, 6227.
38. Momenteau, M.; Scheidt,W. R.; Eigenbrot, C. W.; Reed, C. A. J Am Chem Soc 1988, 110, 1207.
39. Jameson, G. B.; Rodley, G. A.; Robinson, W. T.; Gagne, R. R.; Reed, C. A.; Collman, J. P. Inorg Chem 1978, 17, 850.
40. Jameson, G. B.; Molinaro, F. S.; Ibers, J. A.; Collman, J. P.; Brauman, J. I.; Rose, E.; Suslick, K. S. J Am Chem Soc 1980, 102, 3224.
41. Nurco, D. J.; Medforth, C. J.; Forsyth, T. P.; Olmstead, M. M.; Smith, K. M. J Am Chem Soc 1996, 118, 10918.
42. Deeth, R. J. J Am Chem Soc 1999, 121, 6074.

IV

Theoretical Assessment on the Viability of Possible Intermediates in the Reaction Mechanism of Catalase and Peroxidase Models

Guada Barea, Feliu Maseras, and Agustí Lledós

Unitat de Química Física, Departament de Química, Universitat Autònoma de Barcelona, 08193 Bellaterra, Barcelona, Catalonia, Spain.

Sotmès per a la seva publicació al *Theoretical Chemistry Accounts*

Theoretical assessment on the viability of possible intermediates in the reaction mechanism of catalase and peroxidase models

GUADA BAREA, FELIU MASERAS, AGUSTÍ LLEDÓS
Unitat de Química Física, Edifici C.n, Universitat Autònoma de Barcelona, 08193 Bellaterra, Catalonia, Spain.

ABSTRACT: IMOMM(Becke3LYP:MM3) calculations are performed on different proposed intermediates in the reaction pathway of iomimetic models of catalase and peroxidase enzymes. These calculations allow the identification of their ground state, structural features and relative energies. The relative energies are shown to depend heavily on the nature of the sutrates involved in the reaction, and they are analyzed in detail for the case of the oxidation of alcohol to aldehyde y hydrigen peroxide. All the considered intermediates are found to be within reasonable energy span.

Introduction

A heme group containing a ferric iron center is the common feature of a number of enzymes sharing the ability to catalyze the oxidation of a variety of organic substrates. Among them, one can mention catalases, peroxidases and cythocromes [1,2]. Despite this general oxidative behavior, the particular reaction taking place depends very much on the specific nature of the enzyme and the substrate. The origin of these differences is not fully understood yet, but it must be related to subtle changes in the complicated multistep mechanism of these reactions. A detailed knowledge of the reation mechanism of these enzymes would be thus much desired.

Experimental elucidation of these mechanisms is difficult because of the elusiveness of the eventual intermediates, and the impossibility to characterize the transition states. In any case, some conclusions have already emerged, like the presence of the so-called compounds I and II, at least in some cases. Theoretical chemistry can be helpful in the determination of the mechanisms, but its application has been hampered until very recently by the size of the systems and by its electronic complexity, requiring the application of hight-level, heavily computer demanding methods [3,4]. One must mention however in this concern the continued work by Loew and co-workers on the reaction mechanism of compound I formation in cythocrom c peroxidase [5], and the very recent studies by Shaik and co-workers on the rebound mechanism of hydroxylation by cythocrome P-450 [6].

There is still a wealth of knowledge to be gained from theoretical studies of this type of mechanisms. In this

article, we present a study focused on the behavior of water-soluble iron porphyrins, where one axial ligand is occupied by one water molecule or one hydroxyl ligand, like in Fe(P)(OH) (P=porphyrin). Water-soluble heme complexes, easier to characterize and study [7-10], have been used by a number of authors for the study of oxidation mechanisms, although some questions arise with respect to the coincidence of their mechanism with that of biological systems. Full characterization of a reaction mechanism requires of course the location of the transition sates, but a first step must be the location of the intermediates, corresponding to local energy minima. There are so many possible intermediates for this process that we have found interesting to compute a number of them and discuss their relative energies. These energies will give an idea of their viability and of the place that may occupy in the catalytic cycle.

The calculations use the hibrid QM/MM method IMOMM [11]. This method reduces substancially the computational cost of the calculation by describing part of the system with a molecular mechanics force field, and it has been shown to be efficient in the study of a variety of transition metal systems [12], including some with the heme group [13,14].

Computational details

All calculations throughout this paper have been performed using the IMOMM method with a program built from modified versions of two standard programs: GAUSSIAN 92/DFT [15] for the quantum mechanics part and mm3(92) [16] for the molecular mechanics part. The heme group is modeled in the quantum region as [Fe(NH(CH3)NH)2]. This QM/MM partition has been demonstrated to reproduce well geometrical and electronic parameters of the heme group [13,14].

The QM part of the calculation was done at the density functional theory (DFT)-based unrestricted Becke3LYP level [17]. An effective core potential (ECP) replaced the 10 innermost electrons of the iron atom. The basis set for the Fe was the valence doule-ζ contraction labeled LANL2DZ associated to this ECP. Carbon and hydrogen atoms have been described by the minimal basis set STO-3G, with the exception of the hydrogen atoms bonded to oxygen, which have been described with the 6-31G valence double-ζ basis set. For nitrogen atoms, the 6-31G basis set was used. Two different basis set were used for oxygen. The first of them, which defines basis set I, was 6-31G(d), and was used in most of the geometry optimizations. Basis set II included diffuse functions on oxygen atoms, 6-31+G(d), and was used in one geometry optimization and in single point calculations.

The MM part of the calculations used the mm3(92) force field [18]. Van der Waals parametrs for the iron atom were taken from the UFF force field and torsional contributions involving dihedral angles with the iron atom at the terminal position were set to zero. All geometrical parameters were optimized except the bond distances between the QM and the MM regions of the molecule. The frozen values were 1.019 Å (N-H), 1.101 Å (C-H) in the QM part; and 1.378 Å (N-C), 1.332 Å (C-C) in the MM part. The molecule is oriented in such a way that the porphyrin ring is approximately in the xy plane, and the projections of the Fe-N bonds lie approximately on the bisectors of the x and y axis.

Structures and electronic states

Catalases, peroxidases and related enzymes operate in a complex multistep mechanism, and few definite conclusions are available on the detailed reaction pathway. As a result, there are a numer of proposed intermediates from different studies, both experimental and theoretical [19-21]. In order to compare their relative energies, they have to be computed with methods of comparable quality. In this section, we present our calculations on the eight complexes shown in Figure 1. These eight complexes have been chosen from previous proposals and other reasonable possibilities. All complexes considered are neutral, this has been accomplished through the alternative use of the neutral H_2O or the anionic OH form for the trans axial ligand. Geometry optimizations are carried out with different spin multiplicities, and the most stable one is chosen.

The two first complexes under consideration (**1** and **2**) correspond to the very first proposed intermediates in the reaction pathway of catalases and peroxidases, the high valent iron-oxo species PFe=O known as compound I and compound II [1]. Compound I has also been generally accepted as involved in the reactions catalyzed by cythocromes P-450 [2].

Compound I is two oxidation equivalents above the ferric resting state. Thus, iron has a formal oxidation state of V, and the form considered for complex **1** is (OH)(P)Fe=O. The nature of the electronic ground state of compound I is still now focus of controversy. From a

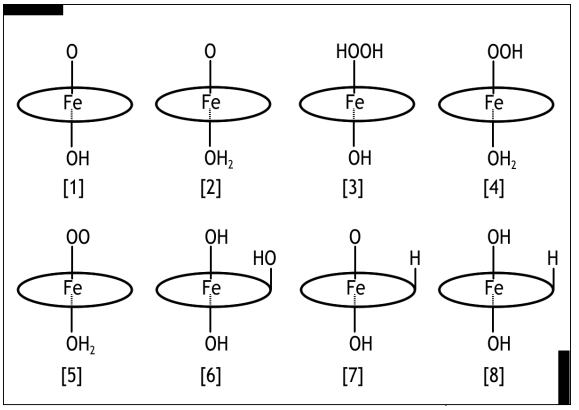

Figure 1. Schematic geometries of the eight complexes under study.

theoretical point of view there is an emerging agreement on the presence of three unpaired electrons (S=3/2) [5,22-26]. Two of the unpaired eletrons are located at the iron-oxo unit and the third one is elsewhere, depending on the model system under consideration, in the porphyrin ring [22-26], in the axial ligand trans to the oxo group [24], or, in some native systems, in a distal amino acid residue [5,27]. In our model, there is no distal amino acid available, and the hydroxylate trans ligand is hardly oxidable. Consequently, we have found a ground state where one electron is removed from the A_{2u} orbital of the porphyrin, in agreement with previous theoretical calculations on models of compound I [5,23-26]. In our model compound I complex **1**, the Fe and O atoms carry spins of 1.29 and 1.06, respectively. The remaining electron is distributed over the porphyrin ring as A_{2u}-type radical, the unpaired spin population on the porphyrin ring being 0.56. The optimized structure of (OH)(P)Fe=O is shown in Figure 2. The Fe-O distance of 1.731 Å is in good agreement with the average distance of *ca.* 1.70 Å found in the X-ray structures of model complexes [28].

Our model for compound II is complex **2**, (H_2O)(P)Fe=O. Compound II is one oxidation equivalent above the ferric resting state, and the iron atom has a formal oxidation state of IV. We have computed electronic states with four different multiplicites for complex **2**: singlet, triplet, quintet and septuplet. Their relative energies are 27.7, 0.0, 15.2 and 25.5 kcal/mol, respectively. The triplet is thus the ground state, in agreement with Mössbauer spectroscopic studies on biomimetic model complexes [29] and previous theoretical studies [23-26,30]. The two unpaired electrons are essentially in the iron-oxo unit, with spin populations of 1.32 on iron and 0.70 on oxygen, a value that is in quite good agreement with that obtained from ENDOR measurements on HRP-I and HRP-II [31]. Our optimized geometry for complex **2** is shown in Figure 2. During geometry optimization, the axial water molecule migrates from its initial bonding location to an iron-water ligand non bonding distance of more than 3 Å, the resulting complex being in fact 5-coordinate. The iron-oxo distance has been found to be 1.621 Å, which is in very good agreement with the result obtained for Fe(T_{piv}PP)O (T_{piv}PP=tetrakis(pivaloyphenyl)porphyrin) through X-ray analysis [32].

Complexes **3** and **4** correspond to intermediates proposed by Poulos and Kraut in the process of formation of compound I in heme peroxidases [20]. Their mechanism starts with the original coordination of hydrogen peroxide to the heme group (complex **3**), and continues through abstraction of one hydrogen atom from the peroxide (complex **4**).

All our attempts to optimize (OH)(P)Fe(HOOH) (complex **3**) as a species containing a strong chemical bond between the heme group and hydrogen peroxide have been unsuccessful. Geometry optimizations in doublet, quartet and sextet states have all converged to structures where the hydrogen peroxide ligand migrates from its initial bonding location to an iron-peroxide non bonding distance of *ca.* 3 Å. We are not aware of previous theoretical calculations on any related system with hydroxylate as trans axial ligands, but some works have been reported with imidazole as trans axial ligand [5,33,34]. Recent Becke3LYP calculations by Siegbahn and co-workers [5] showed in fact that the stable coordination of hydrogen peroxide to heme in model peroxidases required the presence of a hydrogen bond to a distal histidine, which is absent from our system. The P-450 model with a methyl sulfide as trans axial ligand seems on the other hand to bind tightly hydrogen peroxide [36]. Presence of binding depends thus probably on the nature of the trans axial ligand.

The lack of coordination of the hydrogen peroxide in our model complex **3** (OH)(P)Fe(HOOH) does not mean that this species is not interesting. In fact, because of this lack of coordination, it can model the resting state of the catalytic cycle. In our study, the doublet has been found to be the ground state, with the quartet and sextet states 0.2 and 4.0 kcal/mol above respectively. The nature of this ground state seems to depend on the axial ligand, because CASSCF calculations with an imidazole axial ligand have found a sextet ground state [35], while unrestricted Becke3LYP calculations with a methyl mercaptide in axial position have found a doublet ground

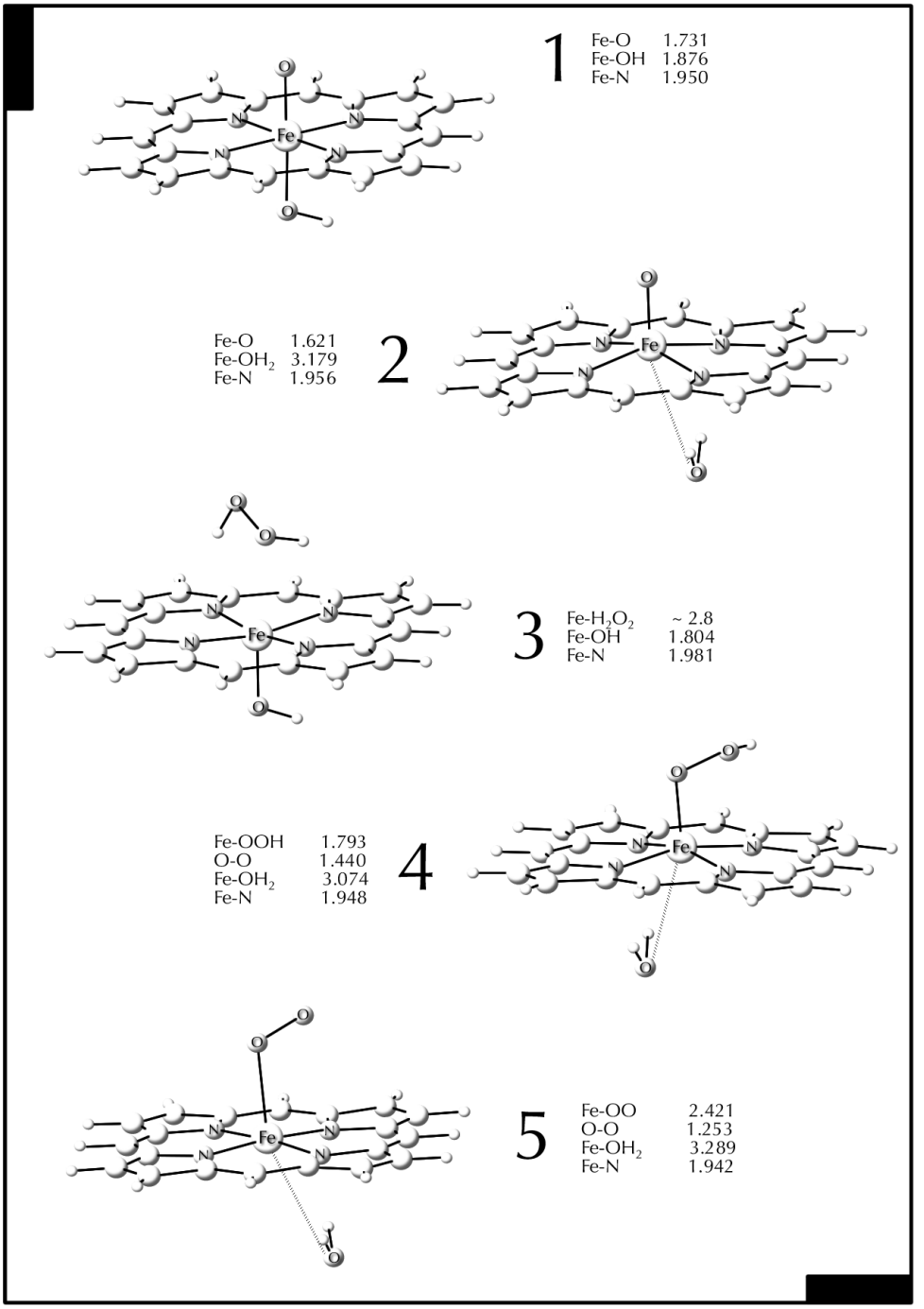

Figure 2. Optimized geometries of complexes (OH)(P)Fe=O (**1**), (H_2O)(P)Fe=O (**2**), (OH)(P)Fe(HOOH) (**3**), (H_2O)(P)Fe(OOH) (**4**) and (H_2O)(P)Fe(O_2) (**5**). Selected distances are given in Å. The average value for the Fe-N bond distance is also provided

state [37]. In fact, anionic ligands have been postulated to stabilize low spin states in ferric complexes [38]. The optimized geometry for complex **3** in its doublet ground state is shown in Figure 2.

Complex **4** contains a OOH unit coordinated to iron, being therefore $(H_2O)(P)Fe(OOH)$. Doublet, quartet and sextet states have been calculated for this compound, and the doublet has been found to be the lowest in energy. Quartet and sextet states have been found to be 3.3 and 16.0 kcal/mol above the ground state respectively. Spin populations on the doublet ground state show that the unpaired electron is mostly located on the iron atom (0.94 spin), mainly on the d_{yz} orbital. These results are in agreement with previous theoretical calculations on analogue model complexes [5,33]. The optimized structure for complex 4 is also shown in Figure 2. The Fe-O distance has been found to be 1.793 Å, and the O-O distance, 1.440 Å.

$(P)Fe(O_2)$ complexes have been postulated as intermediates in the reaction pathway of cythocrome P-450 [36,39,40]. Because of this, we have included $(H_2O)(P)Fe(O_2)$ (complex **5**) in our study. The optimized geometry of this type of complexes is sensitive to the presence of diffuse functions in the oxygen atoms, as we show in a detailed discussion elsewhere [41]. The presentation of the full analysis is out of place in this article, but it can be briefly said that two possible electron arrangements are possible in this system, $Fe^{II}(O_2)$ and $Fe^{III}(O_2^-)$, and in order to properly identify the second of them as the more stable, the anionic nature of the superoxide ligand must be well reproduced. Because of this, diffuse functions on oxygen have been used in this geometry optimization (basis set II). Calculations on singlet, triplet, quintet and septet states have been performed, and found the quintet to be the ground state. Singlet, triplet and septet lie 2.5, 18.6 and 60.4 kcal/mol above respectively. The unpaired electrons are located in the iron atom (2.12 spin) and in the O_2 unit (1.39 spin). The dioxygen unit can be better seen as an O_2^- superoxide, and the Fe-O_2 bond can be thus decribed formally as $Fe^{III}(O_2^-)$, as has been suggested [42]. The optimized geometry for complex **5** is shown in Figure 2. As in other intermediates previously discussed, the water ligand does not bind the heme group.

The last three complexes considered, **6**, **7** and **8** (Figure 3) have one extra substituent in the meso carbon of the porphyrin ring. Although this type of species are not usually considered in the reaction mechanism of catalases and peroxidases, they have been included because of their presence in the degradation process of porphyrins, and because of the biological activity of more saturated derivatives of porphyrin like in F-430 [43].

Our first proposed intermediate with a substituent in the meso carbon is complex **6**, (OH)(POH)Fe(OH), containing two hydroxyl groups as axial ligands and another one in one of the meso carbon atoms. Three different electronic states have been calculated for this compound, doublet, quartet and sextet, with relative energies of 0.0, 17.1 and 20.0 kcal/mol respectively. The doublet is thus the ground state. Spin population analysis of this ground state shows that the only unpaired electron is mostly located on the iron atom (0.87 spin), mainly

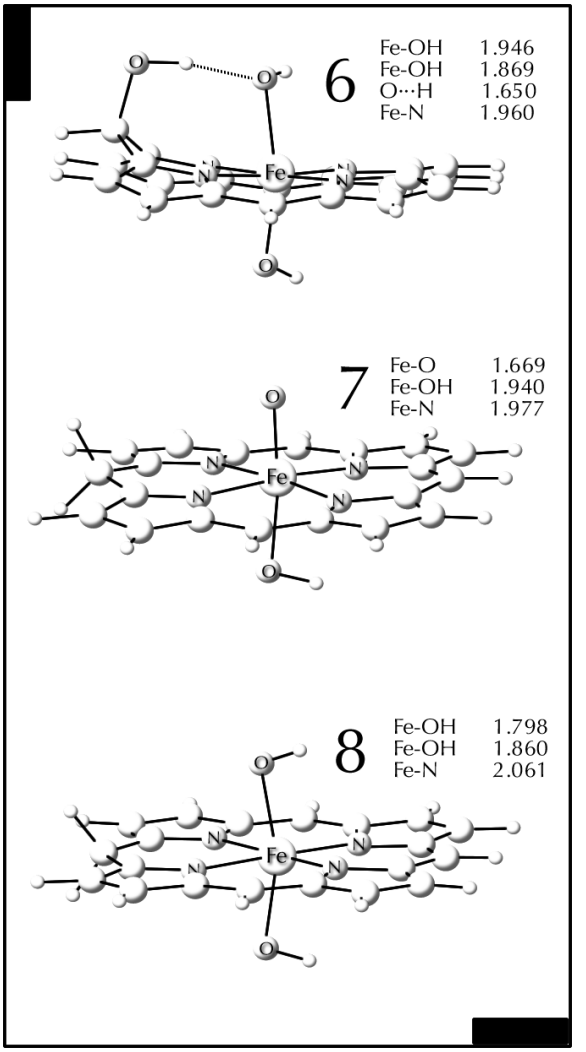

Figure 3. Optimized geometries of complexes (OH)(POH)Fe(OH) (**6**), (OH)(PH)Fe=O (**7**) and (OH)(PH)Fe(OH) (**8**). Selected distances are given in Å. The average value for the Fe-N bond distance is also provided

on the d_{yz} orbital. The optimized geometry is shown in Figure 3. The most remarkable feature of this structure is the presence of a strong hydrogen bond (1.640 Å) between the hydroxyl substituent in the meso carbon and one of the hydroxylate ligands attached to iron. This hydrogen bond is likely to have a direct effect on the reactivity of this intermediate, as will be discussed in the next section.

Complex **7** is (OH)(PH)Fe=O, with an additional hydrogen atom in the meso carbon of porphyrin and an oxo and a hydroxylate groups as axial ligands on iron. Both the electronic structure and the geometry of this complex are quite similar to those of our model for compound II, complex **2**. The system was computed as a triplet with two unpaired electrons on the (pπ-dπ)* molecular orbitals corresponding to the Fe=O group. The spin populations in these atoms are 1.19 for iron and 0.86 for oxygen. The optimized geometry is shown in Figure 3, where it can be seen that the Fe=O distance of 1.669 Å is also very close to that on complex **2** (1.621 Å).

Our last proposed intermediate, complex **8**, (OH)(PH)Fe(OH), has one extra hydrogen atom in a meso carbon, and both axial positions on iron are accupied by hydroxylate ligands. Three different electronic states, doublet, quartet and sextet, were calculated, and again, it was confirmed that the ligation of anionic axial ligands to the Fe(III) center favors the lowest multiplicity. The doublet state was found to be the lowest in energy, with quarted and sextet states 8.6 and 14.3 kcal/mol above respectively. Spin populations show the unpaired electron to be mostly located on the d_{yz} orbital. The optimized structure for the doublet ground state is shown also in Figure 3. The asymmetry between the two Fe-OH bonds (0.062 Å) is remarkable.

Comparision of relative energies

The viability in the reaction of any of the intermediates proposed in the previous section depends critically on their relative energies. The comparision of relative energies is however severely complicated by the fact that not all the compounds have the same number and nature of atoms. All proposed intermediates contain an iron atom and a porphyrin ring, but the number of oxygen and hydrogen atoms differs from one intermediate to another. We propose in this section a simple method to bypass this problem.

The problem of definition of relative nergies comes down to the balancing of a chemical equation. For instance, we cannot compare directly the energies of complexes **6** and **7** (Eq. 1) because they do not have the same number and nature of atoms, and consequently, the chemical equation relating directly both of them (Eq. 1) is not balanced, with one more oxygen atom and one more hydrogen atom on the left side:

$$(OH)(POH)Fe(OH) \; ¢ \; (OH)(PH)Fe{=}O \qquad [1]$$

The method proposed here consists on balancing equations through the addition of the necessary pairs of oxygen donors and/or hydrogen donors until the equation is balanced. In the example just mentioned, this would mean:

$$(OH)(POH)Fe(OH) + d + d' \; ¢ \; (OH)(PH)Fe{=}O + dO + d'H \qquad [2]$$

Where dO/d is an oxygen donor pair, and d'H/d' is a hydrogen donor pair. In this way, the number and nature of the atom in both sides are balanced, and the energies of possible intermediates can be directly compared.

We have used the following pairs as oxygen donors/acceptors:

$$H_2O_2 \; ¢ \; H_2O + O \qquad [A]$$

$$CH_2(O)CH_2 \; ¢ \; CH_2CH_2 + O \qquad [B]$$

$$PhIO \; ¢ \; PhI + O \qquad [C]$$

The pair in reaction **A**, hydrogen peroxide/water, has been included because it is precisely the abstraction of one oxygen atom from hydrogen peroxide the net result of the reaction catalyzed by peroxidases. The pair in reaction **B**, ethylene epoxide/ethylene, is considered because epoxidation of certain substances is one of the reactions catalyzed by water soluble porphyrin ferric complexes [44-46]. Finally, the pair in reaction **C**, iodosylbenzene/iodobenzene, is considered because of its widespread use as oxygen donor including the case of heme-catalyzed epoxidations [47]. The three reactions **A**, **B**, **C** are endothermic, and the associated energy increases are 36.0, 101.7 and 16.7 kcal/mol respectively.

The three pairs used as hydrogen donor/acceptors have been:

H_2O_2 ¢ HOO + H [D]

C_5NH_7 ¢ C_5NH_6 + H [E]

CH_3CH_2OH ¢ CH_3CHO + 2H [F]

The consideration of pairs **D** and **E** is related to their ready presence in the biological environments. The donor in pair **D**, hydrogen peroxide, is definitely present in the reaction media because of its role as oxygen donor mentioned above. Moreover, its hydrogen donor properties must not be very different from those of water, which is also surely present. C_5NH_7 (Figure 4) was used as a model of nicotinamide adenine dinucleotide (NAD). NAD is a usual agent in hydrogen transfer reactions. Finally, pair **F**, ethanol/acetaldehyde, has been included because one of the reactions catalyzed by peroxidases involve precisely this pair. In this latter case, because there is a difference of two hydrogen atoms between reactant and product, an average value of both transfers is obtained dividing by half the energy of the reaction presented. The three reactions **D**, **E**, **F** are endothermic, and the energy changes associated to the transfer of one hydrogen atom are 85.9, 73.4 and 64.2 kcal/mol respectively.

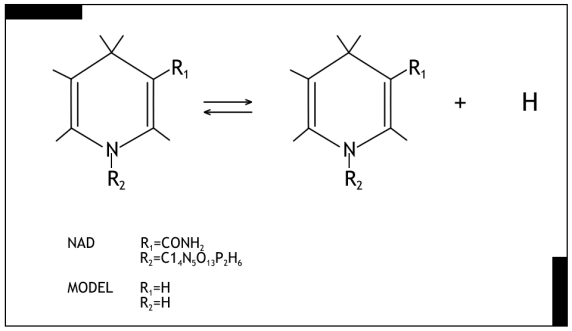

Figure 4. Modelization of the hydrogen donor pair NADH/NAD

Reactions **A** to **F** constitute a representative array of reactions involving the transfer of one single oxygen or hydrogen atoms. Most of the reation steps in biochemical or biomimetical processes of catalase and peroxidase models consist of molecular rearrangements or the transfer of one single atom, but not necessarily all of them. There is certainly the possibility that more than one single atom is transferred in a single step. In particular, the most likely fragments composed of oxygen and hydrogen atoms will be the hydroxyl radical, and the water and the hydrogen peroxide molecules. In order to include this possibility, the following reactions have to be added to the scheme being proposed:

O + H ¢ OH [G]

O + 2H ¢ H_2O [H]

2O + 2H ¢ H_2O_2 [I]

The three reactions **G**, **H**, **I** are clearly exothermic, with values of -103.8, -222.3 and -258.2 kcal/mol respectively. These values will have to be combined with those from equations **A**-**F** in the cases where more than one atom is transferred in a single step.

There is only one additional question to mention before passing to the direct comparision of the energies. It concerns the basis set. All geometry optimizations used the same basis set I, except (H_2O)(P)Fe(O_2) (complex **5**) where, as commented in the previous section, a larger basis set II had been shown to be necessary. In order to make the comparision possible, additional single point calculations using basis set II were carried out on all other complexes on the structures optimized with basis set I.

Results from the application of this method of analysis, assuming all processes to be single atom transfers, to our set of compounds using different oxygen and hydrogen donors are shown in Table 1. The origin of relative energies has been placed in complex **2**, because it corresponds to compound II, the intermediate that is generally accepted for a larger variety of systems. It is clear from the Table that the relative ordering of the species depends critically on the nature of oxygen and hydrogen donor/acceptor pairs being considered. Epoxide (pair **B**) is a very bad oxygen donor, and because of that, it destabilizes the species with more oxygen atoms (three), which are **3**, **4**, **5** and **6**, while iodosylbenzene (pair **C**), which is a strong oxygen donor, stabilizes the same species by a large amount. The differences between the strengh of hydrogen donors are smaller. The stronger donor is ethanol (pair **F**), and the worst is hydrogen peroxide (pair **D**), with the NADH model (pair **E**) in between. The different behavior of iodosylbenzene and epoxide can be readily correlated with the fact that the former will always act as a reactant and the latter always as product in this type of systems. Nevertheless, the Table clearly shows that the relative energies of the intermediates depend on the substrate, and that its nature can affect essentially the mechanism. It must also be mentioned that these energies correspond to the particular (H_2O)Fe(P) model being studied, that all steps are assumed to involve the transfer of no more than one single atom, and that different donor/acceptor pairs can be

used in different steps of the same catalytic process.

In what follows, our discussion will be focused on the energy ordering associated to two particular pairs of oxigen and hydrogen donors, those labeled as A and F, because they correspond precisely to the main reaction catalyzed by peroxidase enzymes, which is exothermic by 57.9 kcal/mol:

$$H_2O_2 + CH_3CH_2OH \; ¢ \; CH_3CHO + 2\ H_2O$$

The span of relative energies is very large with one complex, **8**, 48.0 kcal/mol above **2**; and another one, **6**, 65.1 kcal/mol below **2**. The case of species **6**, which appears to be too stable, deserves some comment.Complex **6** is (OH)(POH)Fe(OH), the intermediate with a hydroxyl group attached to one meso carbon of the porphyrin. A close examination of its optimized structure (Figure 4) shows that there is a strong hydrogen bond between the hydrogen of the hydroxyl group attached to the meso carbon and the oxygen atom of one of the hydroxyl groups attached to the metal. The H···O distance is only 1.650 Å, while the streched O-H bond is as long as 1.025 Å. If the hydrogen transfer insinuated by this strong hydrogen bond were to be completed, a double bond would be formed between the oxygen and the meso carbon, and this would likely lead to the destruction of the porphyrin ring. Remarkably enough, this is in fact a process known to be thermodinamically favorable, and it is therefore not strange to find this complex the most stable. However, this process is likely avoided because of kinetic reasons in the form of high energy barriers which keep tha catalytic cycle out of this undesired path.

A second aspect in Table 1 which deserves specific comment is the high energy of complex **1**, corresponding to compound I, which is 40.8 kcal/mol above complex **2**, and also far above of most of the other proposed species. This result may seem surprising, because compound I had been postulated as an intermediate in related reactions. If the catalitic process were to go through single atom transfers, this species would be out of reach, with an energy 53.9 kcal/mol above the resting state species **3**, which presents a very long iron-oxygen distance. Things become however more reasonable if one takes into account that is generally accepted [5] that a water molecule is eliminated as such during the process going from the resting state to compound I:

$$(OH)(P)Fe(HOOH) \; ¢ \; (OH)(P)Fe{=}O \; + \; H_2O$$

If this is the case, the energies proposed in Table 1 must be shifted for the compounds before this water elimination. For this particular set of donor/acceptor pairs, this means that the relative energies for complex **3** and the closely related complex **4** must be increased by 57.9 kcal/mol. This value is obtained when correcting the value for single atom transfers for the loss of a whole water molecule, and corresponds numerically to the energy gain associated to the process defined by the addition of reactions **A** + **F** + **H**. Thus, the corrected energies for **3** and **4** will be +44.8 kcal/mol and +26.3 kcal/mol respectively.

The resulting picture is that species **1** and **3** have close energies (within 4 kcal/mol), and they can both be present in the catalytic cycle if they are related by a water elimination step. Interestingly enough, both species have an energy high above (*ca.* 40 kcal/mol) of complex **2**, our model for compound II. This suggests a strongly irreversible step for the transformation from compound I to compound II, at least in the oxidation reactions catalyzed by water-soluble iron porphyrins.

The peroxide complex **4**, with a corrected energy of 26.3 kcal/mol above **2** appears as completely reasonable, in agreement with the experimental proposals [8,48,49] of (L)(P)Fe(OOH) intermediates. Another species which from an energetic point of view could be present in the catalitic cycle is **5**, $(H_2O)(P)Fe(O_2)$, which is 25.2 kcal/mol below **2**. This type of species had been proposed to be involved in the reactions catalyzed by cythocrom P-450 [3]. Complex **5** could also have a role even before the water elimination step, in which case its corrected energy would be 32.7 kcal/mol.

The last two computed complexes that remain to be commented, **7** and **8**, have an extra hydrogen attached to the meso carbon. Both of them have energies significantly higher than complex **2**, but reasonably close to **1** or the corrected values for **3** and **4**. Therefore, they can play a role in the reactivity of the system, but it has to be necessarily in the early stages of the reaction, before compound II is reached.

Conclusions

Hybrid QM/MM calculations on eight possible intermediates of the reaction mechanism of water-soluble porphyrin iron complexes modeling catalase and peroxidase enzymes have allowed the identification of their ground state and structural features. The relative energies of these eight prposed complexes have also been evaluated through a scheme involving the consideration of oxygen and hydrogen donors to account for the

Taula 1. Relative energies (kcal/mol) of the eight complexes under study. The oxygen donor pairs are **A**(H_2O_2/H_2O), **B**($CH_2(O)CH_2$)/CH_2CH_2) and **C**(PhIO/PhI) and the hydrogen donor pairs are **D**(H_2O_2/HOO), **E**(C_5NH_7/C_5NH_6) and **F**(CH_3CH_2OH/CH_3CHO). All reactions are assumed to take place through single atom transfers.

different number and nature of atoms in the species under study. The possible elimination of one whole water molecule in one single step has also been considered. The analysis leads to the conclusion that the eight proposed intermediates can play a role in the reactivity of the system. The confirmation of their viability will require an investigation of the reaction paths connecting them. This study is currently under way in our Laboratory.

Acknowledgement. Financial support from the Spanish DGES (Project No. PB98-0916-CO2-01) and the Catalan DURSI (Project No. 19999SGR00089) is acknowledged. F. M. thanks also the support of DURSI (Generalitat de Catalunya).

References

[1] Everse J, Everse K E, Grisham M B (eds) (1991) Peroxidases in Chemistry and Biology. CRC Press:Boca Raton, Ann Arbor, Boston.
[2] Oriz de Montellano P R (ed) (1986) Cythocrome P-450. Structure, Mechanism and Biochemistry. Plenum Press:New York and London.
[3] Loew G H, Harris D L (2000) Chem Rev 100:407.
[4] Siegbahn P E M, Blomberg M R A (2000) Chem Rev 100:421.
[5] Wirstam M, Blomerg M R A, Siegbahn P E M (1999) J Am Chem Soc 121:10178.
[6] (a) Harris N, Cohen S, Filatov M, Ogliaro F, Shaik S (2000) Angew Chem Int Ed Engl 39:2003. (b) Ogliaro F, Harris N, Cohen S, Filatov M, deVisser S P, Shaik S (2000) J Am Chem Soc 122:8977.
[7] Lee J, Hunt J A, Groves J T (1998) J Am Chem Soc 120:7493.
[8] Sisemore M F, Burstyn J N, Valentine J S(1996) Angew Chem Int Ed Engl 35:206.
[9] Song R, Sorokin A, Bernadou J, Meunier B (1997) J Org Chem 62:673.
[10] Dorovska-Taran V, Posthumus M A, Boeren S, Boersma M G, Teunis C J, Rietjens I M C M, Veeger C (1998) Eur J Biochem 253:659.
[11] Maseras F, Morokuma K (1995) J Comput Chem 16:1170.
[12] (a) Maseras F (1999) Top Organomet Chem 4:165. () Maseras F (2000) Chem Comm 1821.
[13] Maseras F (1998) New J Chem 22:327.
[14] Maréchal J -D, Barea G, Maseras F, Lledós A, Mouaward L, Pérahia D (2000) J Comput Chem 21:282.
[15] Frisch M J, Trucks G W, Schlegel H B, Gill P M W, Johnson B G, Wong M W, Foresman J B, Robb M A, Head-Gordon M, Replogle E S, Gomperts R, Andres J L, Raghavachari K, Binkley J S, Gonzalez C, Martin R L, Fox D J, Defrees D J, Baker J, Stewart J J P, Pople J A Gaussian 92/DFT, Gaussian Inc:Pittsburg PA, 1993.
[16] Allinger N L mm3(92) (1992) QCPE:Bloomington IN.
[17] Stephens P J, Devlin F J, Chavalowski C F, Frish M J (1994) J Phys Chem 98:11623.
[18] Allinger N L, Yuh Y H, Lii J H (1989) J Am Chem Soc 111:8551.
[19] Strich A, Veillard A (1983) Nouv J Chim 7:347.
[20] Poulos T L, Kraut J (1980) J Biol Chem 225:8199.
[21] Ozaki S, Inada Y, Watanabe Y (1998) J Am Chem Soc 120:8010.
[22] Loew, G H, Axe F U, Collins J R, Du P (1991) Inorg Chem 30:2291.
[23] Kuramochi H, Noodleman L, Case D A (1997) J Am Chem Soc 119:11442.
[24] Antony J, Grodzicki M, Trautwein A X (1997) J Phys Chem A 101:2692.

[25] Yamamoto S, Kashiwagi H (1998) Chem Phys Lett 145:111.
[26] Ghosh A, Almlöf, J, Que L Jr (1994) J Phys Chem 98:5576.
[27] Jensen G M, Bunte S W, Warshel A, Goodin D B (1998) J Phys Chem B 102:8221.
[28] Collman J P, Gagne R P, Reed C A, Robinson W T, Rodley G A (1976) Proc Natl Acad Sci USA 71:1326.
[29] (a) Boso B, Lang G, McMurray T J, Groves T J (1983) J Chem Phys 79:1122. (b) Gold A, Jayaraj K, Doppelt P, Weiss R, Chottard G, Bill E, Ding X -Q, Trautwein A X (1988) J Am Chem Soc 110:5756.
[30] (a) Penner-Hahn J E, McMurray T J, Renner M, Latos-Grazinsky L, Smith-Eble K, Davis I M, Balch A L, Groves J T, Dawson J H, Hodgson K O (1983) J Biol Chem 258:12761. (b) Penner-Hahn J E, Smith-Eble K, McMurray T J, Renner M, Balch A L, Groves J T, Dawson J H, Hodgson K O (1986) J Am Chem Soc 108:7819.
[31] (a) Penner-Hahn J E, McMurray T J, Renner M, Latos-Grazinsky L, Smith-Eble K, Davis I M, Balch A L, Groves J T, Dawson J H, Hodgson K O (1983) J Biol Chem 258:12761. (b) Penner-Hahn J E, Smith-Eble K, McMurray T J, Renner M, Balch A L, Groves J T, Dawson J H, Hodgson K O (1986) J Am Chem Soc 108:7819.
[32] Shappacher M, Weiss R, Montiel-Montoya R, Trautwein A, Tabard A (1985) J Am Chem Soc 107:3736.
[33] Harris D L, Loew G H (1996) J Am Chem Soc 118:10588.
[34] Loew G, Dupuis M (1996) J Am Chem Soc 118:10584.
[35] Loew G, Dupuis M (1997) J Am Chem Soc 119:9848.
[36] Harris D L, Loew G H (1998) J Am Chem Soc 120:8941.
[37] Green M T (1998) J Am Chem Soc 120:10772.
[38] Axe F U, Flowers C, Loew G H, Waleh A (1989) JAm Chem Soc 111:7333.
[39] Dawson J H, Sono M (1987) Chem Rev 87:1255.
[40] Harris D, Loew G, Waskell L (1998) J Am Chem Soc 120:4308.
[41] Barea G, Maseras F, Lledós A (2001) Int J Quantum Chem 85 2:100 .
[42] Momenteau M, Reed C A (1994) Chem Rev 94:659.
[43] Zimmer M, Cratree R H (1999) J Am Chem Soc 121:1062.
[44] Lee K A, Nam W (1997) J Am Chem Soc 119:1916.
[45] Yang S J, Nam W (1998) Inorg Chem 37:606.
[46] Bernadou J, Fabiano A -S, Robert A, Meunier B (1994) J Am Chem Soc 116:9375.
[47] Groves J T, Haushalter R C, Nakamura M, Nemo T E, Evans B J (1981) J Am Chem Soc 103:2884.
[48] Selke M, Valentine J S (1998) J Am Chem Soc 120:2652.
[49] Ho R Y N, Roelfes G, Hermant R, Feringa B L, Que L Jr. (1999) Chem Commun 2161.

V

Unexpectedly Large Basis Set Effects on the Binding of O_2 to Heme Complexes

Guada Barea, Feliu Maseras, and Agustí Lledós

Unitat de Química Física, Departament de Química, Universitat Autònoma de Barcelona, 08193 Bellaterra, Barcelona, Catalonia, Spain.

International Journal of Quantum Chemistry

2001 Volume 85, Pages 100-108

Unexpectedly Large Basis Set Effects on the Binding of O_2 to Heme Complexes

GUADA BAREA, FELIU MASERAS, AGUSTÍ LLEDÓS

Unitat de Química Física, Edifici C.n, Universitat Autònoma de Barcelona, 08193 Bellaterra, Catalonia, Spain

Received 12 July 2000; revised 7 May 2001; accepted 21 May 2001

ABSTRACT: IMOMM(Becke3LYP:MM3) geometry optimizations on the $Fe(P)(H_2O)(O_2)$ (P = porphyrin) system with different basis sets are shown to provide large differences in the iron–oxygen bond distance. This difference is found to be not in the basis set superposition error or in the description of the interaction between iron and dioxygen. Instead, the origin of the difference is shown to be in the relative energies of the $Fe^{II}(P)(O_2)$ and $Fe^{III}(P)(O_2^-)$ descriptions emerging from the stabilities of the separate Fe^{II}/O_2 and Fe^{III}/O_2^- fragments. © 2001 John Wiley & Sons, Inc. Int J Quantum Chem 85: 100–108, 2001

Key words: heme complexes; density functional methods; basis set superposition error; heme–dioxygen interaction; bioinorganic chemistry

Introduction

The interaction between dioxygen units and heme groups plays a key role in the biological activity of a number of relevant proteins and enzymes, such as hemoglobin, myoglobin, catalases, peroxidases, and cytochromes [1–3]. This interaction is quite subtle, because a wide variety of behaviors are observed depending on the protein environtment. For instance, transport proteins mioglobyn and hemoglobyn contain Fe^{II} in its deoxygenated state, and do not lead to scission of the oxygen–oxygen bond. On the contrary, catalase and peroxidase enzymes contain Fe^{III} in its resting state, and are involved in reactions where oxygen–oxygen bonds are broken.

A productive experimental approach to the understanding of the reaction mechanism of catalases and peroxidases has been provided by the study of water soluble iron porphyrins [4–7]. Although these complexes do not necessarily follow the same reaction patterns of their biological counterparts, they seem to mimic some of their reaction steps, providing much needed information on these complicated mechanisms. There is, however, a certain controversy on their detailed reaction mechanism [5–7], and a theoretical study could be helpful in this context.

The theoretical study of heme complexes has long drawn the attention of theoretical che-

Correspondence to: G. Barea; e-mail: ada@klingon.uab.es.
Contract grant sponsor: Spanish DGESIC.
Contract grant number: PB98-0916-CO2-01.
Contract grant sponsor: Catalan DGR.
Contrant grant number: 1999SGR00089.

mists [8, 9]. However, efforts have been hampered by the size and the complexity of the systems, and the ab initio theoretical study of heme groups has become widespread only in recent years [10–25], because of the increase in computer power, and because of the appearance of new methodologies. In particular, we have already applied with success the IMOMM method [26] to this type of system [17, 25]. IMOMM is a hybrid quantum mechanics/molecular mechanics (QM/MM) scheme that allows the accurate study of large systems with a much lower computational effort, as proved by its many applications in transition metal chemistry [27].

With these ideas in mind we decided to study the interaction of water soluble porphyrins with oxygen with the IMOMM method. In particular we considered the Fe(P)(H_2O)(O_2) (P = porphyrin) complex in order to study its reactivity. The water molecule was added as potential axial ligand to the iron group, although its experimental role is under discussion, and all our calculations indicated that in fact it does not bind to iron. The iron atom in the resulting species was therefore five-coordinate, with four bonds to the heme group and one to the dioxygen subunit. We found in these calculations, to our surprise, that the nature of the optimized geometry obtained was very much dependent on the basis set, with large geometrical changes associated to seemingly small basis set changes. This problem can have a decisive effect in the theoretical analysis of this type of system, and because of that we decided to analyze it in detail. This article presents the results of this analysis.

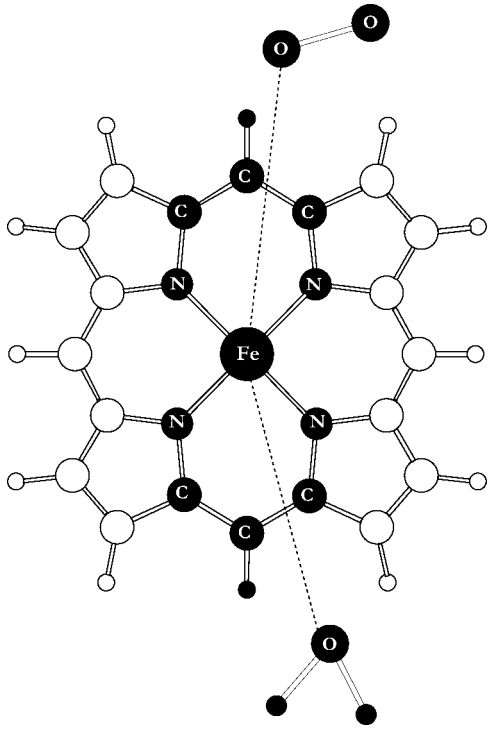

FIGURE 1. QM/MM partition used in the calculations. Atoms in the QM part are depicted in black.

Computational Details

All calculations throughout this article have been performed using the IMOMM method with a program built from modified versions of two standard programs: Gaussian 92/DFT [28] for the quantum mechanics part and mm3(92) [29] for the molecular mechanics part. The QM/MM partition is shown in Figure 1, where the quantum mechanics region is defined by the atoms in black. Thus, the heme group is modeled in the quantum region as [Fe(NH(CH_3)$_3$NH)$_2$]. This QM/MM partition has been demonstrated to reproduce well geometrical and electronic parameters of the heme group [17, 25].

The QM part of the calculation was done at the density functional theory (DFT)-based unrestricted Becke3LYP level [30]. A quasirelativistic effective core potential (ECP) replaced the 10 innermost electrons of the iron atom. The basis set for Fe was always the valence double-ζ contraction labeled LANL2DZ associated to this ECP. A variety of basis sets, including STO-3G, 6-31G, 6-31G(d), 6-31+G, and 6-31+G(d) were used for the other atoms, the particular set applied in each case being indicated in Table I.

The MM part of the calculations used the mm3(92) force field [31]. Van der Waals parameters for the iron atom were taken from the UFF force field and torsional contributions involving dihedral angles with the iron atom at the terminal position were set to zero. All geometrical parameters were optimized except the bond distances between the QM and the MM regions of the molecule. The frozen values were 1.019 Å (N—H), 1.101 Å (C—H) in the QM part; and 1.378 Å (N—C), 1.332 Å (C—C) in the MM part. Atom numbering is shown in Figure 2. The molecule is oriented in such a way that the porphyrin ring is approximately in the *x*,*y* plane, and the projections of the Fe—N bonds lie approximately on the bisectors of the *x* and *y* axis.

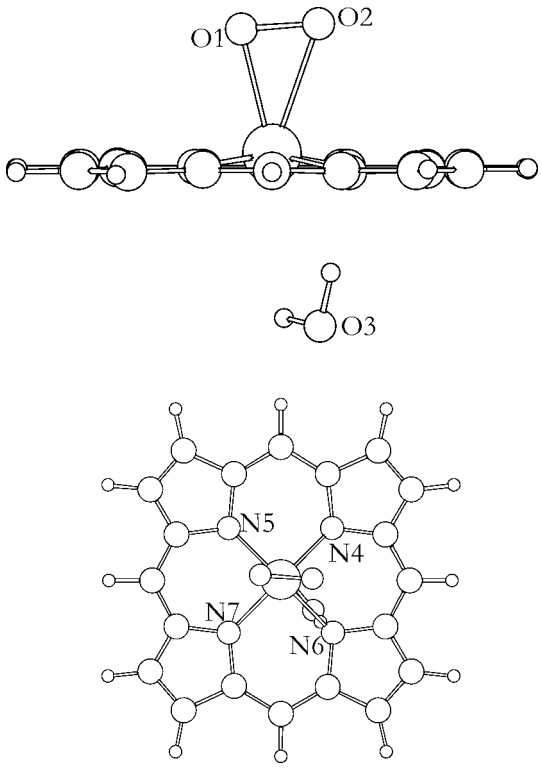

FIGURE 2. Two views of the IMOMM(Becke3LYP:MM3) optimized geometry of the [Fe(P)(H_2O)(O_2)] complex with basis set I.

Binding of O_2 to Fe(P) Depends on the Basis Set

To our knowledge, no conclusive experimental evidence is available for the electronic structure of Fe(P)O_2 complexes. From a theoretical point of view, there have been different proposals for the nature of the ground state, including a triplet and an open shell singlet [13, 26]. Thus, we performed calculations on singlet (S = 0), triplet (S = 1), quintet (S = 2), and septet (S = 3) states with the small basis set labeled as I. In this basis set, the oxygen atoms are described by valence double-ζ 6-31G basis, while most of the other atoms, including the nitrogen atoms attached to the metal, are described by the minimal STO-3G basis set. The quintet state was found to be the lowest in energy with the triplet, singlet and septet having energies 2.5, 18.6, and 60.4 kcal/mol above, respectively. Spin contamination, measured through the expectation value of S^2, was in all cases small. Our prediction of a quintet ground state for this system is not in agreement with previous theoretical proposals [13, 32]. Discrepancies are probably associated with the different QM levels applied. In any case, even if the ground state was not the quintet we consider here, the discussion that follows on basis sets would still be relevant. The goal of this work is not to carry out calculations on every state, but to show a large basis set effect in one of them, an effect that will likely be present in other cases.

The electronic state found in most of these calculations, with the exception only of the singlet state, had an unpaired electron on the O_2 ligand, on the π^* orbital perpendicular to the plane defined by the iron and the two oxygen atoms, the other π^* orbital being doubly occupied. The other unpaired electrons were located on the iron atom. In the quintet ground state (the only one that will be discussed in what follows), the other three unpaired electrons were located on the d_{z^2}, d_{xy}, and d_{yz} orbitals. Thus the Fe—O_2 bond can be formally described as Fe^{III}—O_2^-, as several experiments have suggested [3].

Figure 2 shows the optimized geometry obtained for the quintet state, and relevant geometrical parameters are collected in Table II. The first thing to note is that the water ligand is very weakly bound to the heme group. The oxygen atom from the water ligand is at a nonbonding distance of 3.175 Å from the metal, so the iron atom is better seen as five-coordinated. This is not unexpected, since it is well

TABLE I
Basis sets used in the optimization of the [Fe(P)(H_2O)(O_2)] system.

	Basis set I	Basis set II	Basis set III	Basis set IV	Basis set V	Basis set VI	Basis set VII
Fe	LANL2DZ	LANL2DZ	LANL2DZ	LANL2DZ	LANL2DZ	LANL2DZ	LANL2DZ
N	STO-3G	6-31G	6-31G	6-31G(d)	6-31G(d)	6-31G	6-31G
O	6-31G	6-31G(d)	6-31G	6-31G	6-31G(d)	6-31+G	6-31+G(d)
$H_{bound\ to\ O}$	STO-3G	6-31G	6-31G	6-31G	6-31G	6-31G	6-31G
Rest	STO-3G	STO-3G	STO-3G	STO-3G	STO-3G	STO-3G	STO-3G

TABLE II

Selected geometrical parameters (Å and degrees) from the geometry optimization of [Fe(P)(H_2O)(O_2)] at the IMOMM(Becke3LYP:MM3) level of calculation with basis sets I to VII.[a]

	Basis set I	Basis set II	Basis set III	Basis set IV	Basis set V	Basis set VI	Basis set VII
Fe—O1	2.243	2.782	2.234	2.248	3.060	2.187	2.421
Fe—O2	2.409	3.325	2.962	2.341	3.524	3.032	3.156
Fe—O3	3.173	3.114	3.181	3.189	3.078	3.299	3.289
O1—O2	1.356	1.226	1.329	1.348	1.218	1.343	1.253
Fe—O1—O2	79.8	105.4	1.098	76.7	101.7	116.4	114.7

[a] Atom labeling is that shown in Figures 2 and 3.

known that the water ligand is a very poor ligand in this type of complex. The porphyrin ring is almost planar, with a deviation from plane of 0.019 Å. The iron displacement from the plane defined by the porphyrin ring is 0.251 Å, which is consistent with this five-coordinate description. Bonding distances between the iron atom and the two oxygen atoms from the dioxygen ligand are 2.244 Å and 2.409 Å, which corresponds to a η^2-coordination. Iron-dioxygen interaction is optimized when the O_2 ligand is oriented parallel to the bisector of the angle defined by N4–Fe–N6 atoms.

The results of these preliminary calculations with the small basis set I were reasonable. We tried afterwards to refine the calculations on the quintet state by using the larger basis set II, where the description for the nitrogen atoms was upgraded from STO-3G to 6-31G, and that for the oxygen atoms from 6-31G to 6-31G(d).

Results (presented in Table II and Figure 3) were surprising because the small change in the basis set completely changed the geometry. In the optimized geometry with basis set II, the O_2 ligand does not bind the heme group, the closest iron–oxygen distance being of 2.782 Å. This change on the system geometry is the reflection of changes in the electronic state. With basis set II, two unpaired electrons are located on the O_2 ligand, on the π^* orbitals. This electronic configuration corresponds to a neutral free dioxygen molecule. This fact is in agreement with the O—O distance found: 1.226 Å, to be compared with 1.220 Å obtained on free dioxygen using the same 6-31G(d) basis set. The remaining two unpaired electrons are located on the iron d_{z^2} and d_{yz} orbitals. Thus we can formulate this system formally as Fe^{II}—O_2. Also the mode of coordination of the O_2 ligand to the heme group has changed. On this geometry optimization two different Fe—O distances are found: 2.791 and 3.334 Å, which is consistent with an η^1-coordination, further confirmed by the Fe—O—O angle of 105.4°. Iron displacement from the porphyrin plane is very close to zero (0.037 Å), a value that corresponds to a four-coordinate geometry.

None of the attempts of geometry optimization keeping the Fe^{III}—O_2^- state with basis set II, as well as those to optimize the Fe^{II}—O_2 state with basis set I, were successful. Furthermore, we tried to fol-

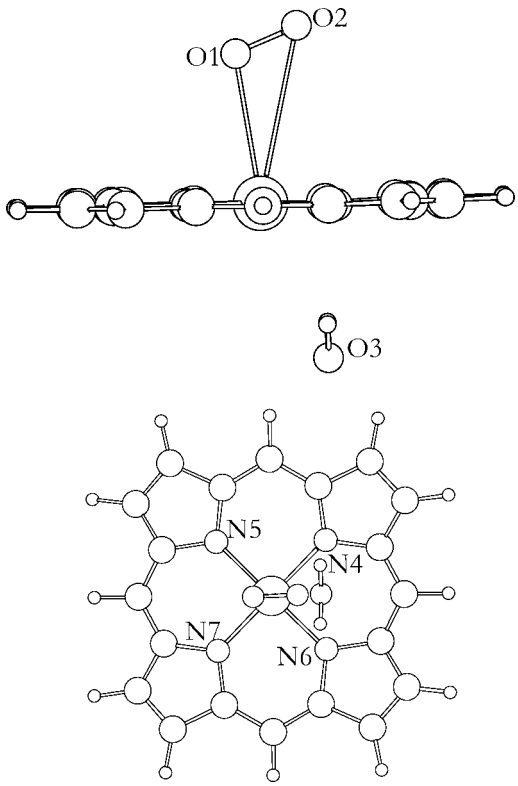

FIGURE 3. Two views of the IMOMM(Becke3LYP:MM3) optimized geometry of the [Fe(P)(H_2O)(O_2)] complex with basis set II.

low the two different states by decreasing the Fe—O distance from the isolated fragments (Fe(P)+O_2) but this attempt was not succesful either. It therefore became clear that the apparently similar basis sets I and II provide a sharply different description of the Fe—O_2 interaction in these complexes.

The Key Difference is the Basis Set on the Oxygen Atoms

The fact that changes in the basis set description of oxygen and nitrogen brought such substantial geometrical changes prompted us to explore the effect of alternative descriptions of these atoms in the geometry optimization of the quintet state. Because of this, basis sets III to VII (Table I) were tested.

We first wanted to examine the influence of the nitrogen basis set on the electronic configuration of the Fe(P)(H_2O)(O_2) system. In order to do this, calculations were carried out using basis sets III and IV. Both use the valence double-ζ 6-31G description on the oxygen atoms as in basis set I, and differ in the description of the nitrogen atoms. In basis set III, valence double-ζ 6-31G is used instead of STO-3G, while in basis set IV, the 6-31G basis is extended with a *d* polarization shell. Relevant geometrical parameters from these two geometry optimizations are shown in Table II.

Results with basis sets III and IV are much more similar to those obtained with basis set I than to those of basis set II. Both basis sets III and IV describe the system as five-coordinate Fe^{III}—O_2^-, with an unpaired electron located on the O_2 ligand and three unpaired electrons located on the iron orbitals. The only significant difference between calculations performed with basis sets I, III, and IV arises from the O_2 coordination mode. While optimizations from basis sets I and IV present a η^2-coordinated O_2 ligand (Fe—O—O angle of 79.8°, 76.7°), optimizations from basis set III present the O_2 ligand clearly η^1-coordinated (Fe—O—O angle of 109.8°). Therefore, the basis set on nitrogen has some effect on O_2 coordination, but is definitely not responsible for the changes we found between basis sets I and II.

The difference between the optimized geometries with basis sets I and II is thus associated to the different description of oxygen. This was further confirmed by new calculations with basis sets V, VI, and VII presented also in Table II. Because of the anionic character of the O_2 moiety, adding diffuse functions to the oxygen atoms description seems reasonable. Thus, basis sets VI and VII include them. What we found on these calculations is that the inclusion of polarization on the oxygen basis set leads to the dissociation of the O_2 ligand from the heme group, while the inclusion of diffuse functions favor the Fe—O_2 binding, shortening the Fe—O distance.

Results from all tested basis sets indicate that the basis set on the oxygen atoms is the key reason for the different results obtained with basis sets I and II. However, the origin of this effect is not clear, and it is particularly disturbing that the smaller basis set I gives results in better agreement with the largest basis set VII than the more extended basis set II.

Basis Set Superposition Error Analysis

An important factor on the calculation of binding energies of fragments is basis set superposition error (BSSE). This term becomes critical when binding energies are small or when unbalanced basis sets are used. Thus, binding of O_2 to heme in our Fe(P)(H_2O)(O_2) system seems susceptible of having an important BSSE.

Calculation of BSSE for basis sets I and II was our next step in this study. In order to know if BSSE was the responsible for the sharp difference in the Fe—O distances obtained in the geometry optimizations with basis sets I and II, we carried out counterpoise calculations with both basis sets. The question is further complicated here because, as pointed out above, the formal description of the system is Fe^{III}—O_2^- in the optimized geometry with basis set I, and Fe^{II}—O_2 in the optimized structure with basis set II, thus requiring two different counterpoise calculations, two with each basis set. First, the BSSE was computed with basis set I, at the geometry optimized with this same basis set I, and with a Fe(P)(H_2O)$^+$+O_2^- partition. This calculation, yielded a binding energy of −141.0 kcal/mol, which will be labeled as $(\Delta E_{f\text{-}o})_I$ (formation in the oxidized state of Fe with basis set I). The BSSE associated to this interaction was −17.6 kcal/mol $(BSSE_{f\text{-}o})_I$. Second, the BSSE was computed with basis set II, at the geometry optimized with this same basis set II, and with a Fe(P)(H_2O) + O_2 partition. The resulting interaction energy $(\Delta E_{f\text{-}r})_{II}$ was −3.0 kcal/mol, with an associated $(BSSE_{f\text{-}r})_{II}$ of −2.9 kcal/mol. Neither the binding energies nor the basis set superposition error computed in this way can be directly compared. The problem is that the interaction between the charged Fe(P)(H_2O)$^+$ + O_2^- fragments is much stronger than when the fragments are neutral, mostly because of the large electrostatic interaction.

TABLE III

IMOMM and pure QM calculated values (kcal/mol) for the $\Delta E_{d\text{-}t}$, $\Delta E_{f\text{-}r}$, $\Delta E_{f\text{-}o}$, and $\Delta E_{o\text{-}r}$ terms for basis sets I and II. Associated BSSE for the IMOMM values are also shown.

		$\Delta E_{d\text{-}t}$	$-\Delta E_{f\text{-}r}$	$-BSSE_{f\text{-}r}$	$\Delta E_{f\text{-}o}$	$BSSE_{f\text{-}o}$	$\Delta E_{o\text{-}r}$
IMOMM	Basis set I	123.0	5.5	5.0	-141.0	-17.6	-12.6
	Basis set II	157.4	3	2.9	-149.7	-17.6	10.7
Pure QM	Basis set I	122.3	2.5		-137.9		-10.9
	Basis set II	146.3	4.7		-139.5		9.3

In order to make comparisons possible, two additional calculations had to be carried out: $(\Delta E_{f\text{-}r})_I$, where basis set I was applied to the geometry obtained for the reduced iron geometry obtained with basis set II, and $(\Delta E_{f\text{-}o})_{II}$ where basis set II is applied to the structure optimized with basis set I. The results, included in Table III, were -5.5 kcal/mol for $(\Delta E_{f\text{-}r})_I$, and -149.7 kcal/mol for $(\Delta E_{f\text{-}o})_{II}$. The corresponding values for BSSE were -5.0 kcal/mol for $(BSSE_{f\text{-}r})_I$ and -17.6 kcal/mol for $(BSSE_{f\text{-}o})_{II}$. These results indicate that BSSE plays a very minor role in this particular problem. $BSSE_{f\text{-}o}$ is identical (-17.6 kcal/mol) for both basis sets, and has a difference of only 2.1 kcal/mol (-5.0 vs. -2.9 kcal/mol) in $BSSE_{f\text{-}r}$. However, the energy difference between both geometries, which can be labeled as $\Delta E_{o\text{-}r}$, is -12.6 kcal/mol for basis set I $[(\Delta E_{o\text{-}r})_I]$ and $+10.7$ kcal/mol for basis set II $[(\Delta E_{o\text{-}r})_{II}]$. Therefore, there is a difference of 23.3 kcal/mol, which cannot be explained by basis set superposition error. In fact, this difference in $\Delta E_{o\text{-}r}$ stabilities cannot be explained by differences in $\Delta E_{f\text{-}o}$ and $\Delta E_{f\text{-}r}$ values presented above. The origin of the difference has to be in the relative energies of the electronic states of the separate fragments, as can be seen in the thermodynamical cycle presented in Figure 4. This term will be analyzed in detail in the next section.

Stability of the Separate Fe(P) and O_2 Fragments

The $\Delta E_{o\text{-}r}$ energy difference between the two different geometries with a given basis set is, as shown in Figure 4 and Table III, the sum of three terms: $\Delta E_{f\text{-}o}$, $-\Delta E_{f\text{-}r}$, and $-\Delta E_{d\text{-}t}$. $\Delta E_{d\text{-}t}$ stands for the energy difference between the separated reactants at the two different electronic states, a process which involves a geometrical distortion of both fragments and an electron transfer from one fragment to the other, $\Delta E_{f\text{-}o}$ stands for the energy associated with the formation of the complex in the oxidized state of Fe, while $\Delta E_{f\text{-}r}$ is the energy associated with the formation of the complex in the reduced state of Fe. The computed value for $(\Delta E_{d\text{-}t})_I$ is 123.0 kcal/mol, and that of $(\Delta E_{d\text{-}t})_{II}$ is 157.4 kcal/mol. The absolute value is large in both cases, but this is consistent with the natural trend to keep noninteracting fragments as neutral. More significantly to the topic under discussion, the difference between $(\Delta E_{d\text{-}t})_I$ and $(\Delta E_{d\text{-}t})_{II}$ is 34.4 kcal/mol, a value which is the driving force behind the difference of 23.3 kcal/mol between $(\Delta E_{o\text{-}r})_I$ and $(\Delta E_{o\text{-}r})_{II}$, which is in turn marking the nature of the most stable geometry for a given basis set. Therefore, the $\Delta E_{d\text{-}t}$ term is the one that accounts for the different nature of the optimized geometries with both basis sets. The difference is not in the description of the interaction between the fragments but from the description of the fragments themselves. The prefer-

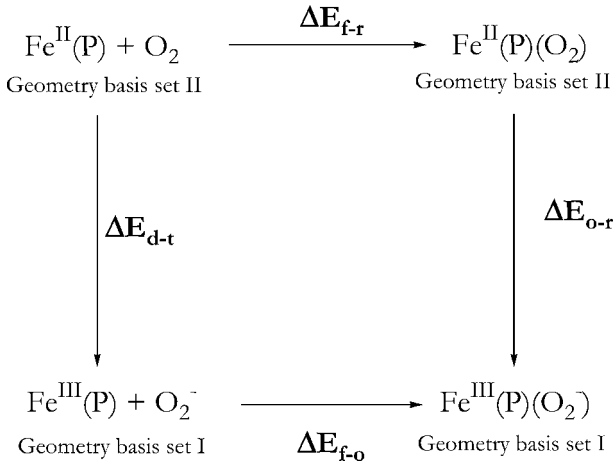

FIGURE 4. The proposed termodynamic cycle for the definition of $\Delta E_{d\text{-}t}$, $\Delta E_{f\text{-}r}$, $\Delta E_{f\text{-}o}$, and $\Delta E_{o\text{-}r}$ terms.

ence of the potentially transferred electron in being on one fragment or the other decides the nature of the most stable structure, and this preference depends heavily on the basis set.

Basis sets I and II provide very different values for the $\Delta E_{\text{d-t}}$ magnitude. The electron transfer from the Fe(P)(H_2O) fragment to the O_2 fragment is easier in basis set I than in basis set II. This is the reason why basis set I leads to the Fe^{III}—O_2^- product while basis set II leads to the Fe^{II}—O_2 product.

The study can be taken one step further by analyzing where the difference in the values for $\Delta E_{\text{d-t}}$ comes from. The value of the $\Delta E_{\text{d-t}}$ magnitude can be decomposed in two contributions: $\Delta E_{\text{d-t}}$(Fe) and $\Delta E_{\text{d-t}}(O_2)$; where each contribution corresponds to one fragment. For basis set I, $[\Delta E_{\text{d-t}}(\text{Fe})]_{\text{I}}$ is 123.7 kcal/mol and $[\Delta E_{\text{d-t}}(O_2)]_{\text{I}}$ is −0.7 kcal/mol. The corresponding values for $[\Delta E_{\text{d-t}}(\text{Fe})]_{\text{II}}$ and $[\Delta E_{\text{d-t}}(O_2)]_{\text{II}}$ are 144.1 and 13.4 kcal/mol. In view of these numbers, this decomposition does not look very useful, because it comes out that basis set I and basis set II provide significantly different values for each of the terms. The analysis becomes clear, however, when additional basis sets are considered. In particular we computed $\Delta E_{\text{d-t}}$(Fe) with five different basis sets differing only in the description of the nitrogen atoms. The basis sets considered for N were STO-3G, 6-31G, 6-31G(d), 6-31+G, and 6-31+G(d). The results for $\Delta E_{\text{d-t}}$(Fe) were 123.7, 140.8, 143.2, 145.5, and 148.0 kcal/mol, respectively. The general trend is the expected one, with the larger basis set stabilizing more the neutral Fe^{II} complex, with one more electron, and increasing the energy gap. However, the increases do not have the same numeric effect. It can be seen that while the STO-3G description yields a value ca. 20 kcal/mol smaller than the others, the other four basis sets yield values concentrated in a narrow span of 6.2 kcal/mol. Therefore, it can be concluded that while a double-ζ description of N is required, addition of polarization and diffuse functions has only a minor effect.

A similar analysis was performed for the $\Delta E_{\text{d-t}}(O_2)$ term with the same basis sets for oxygen that were used before for nitrogen: STO-3G, 6-31G, 6-31G(d), 6-31+G, and 6-31+G(d). The resulting values for $\Delta E_{\text{d-t}}(O_2)$ were: +144.4, −0.7, +13.4, −26.0, and −13.7 kcal/mol, respectively. The numerical dispersion of values is much larger for this term. Here, the STO-3G value is very far from the rest, which is indicative of a poor description with this minimal basis set. However, and in contrast with what happened for $\Delta E_{\text{d-t}}$(Fe), in the case of $\Delta E_{\text{d-t}}(O_2)$ both polarization and diffuse functions have effects larger than 10 kcal/mol on the energy gap between the two frozen geometries being considered. Diffuse functions, which are known to be required for the correct description of anions, stabilize the superoxide anion by 25.3 kcal/mol with respect to the neutral dioxygen. Polarization functions stabilize instead the neutral system by 14.1 kcal/mol. This effect seems related rather to the geometrical distortion than to the change in the system, with polarization functions favoring the system with the shorter O–O distance. In any case, it becomes clear that a proper description will require the use of both polarization and diffuse functions on the atoms of the O_2 ligand. The importance of a good basis set description for oxygen atoms in the characterization of metal–dioxygen interactions had been previously reported in the case of alkali-metal superoxide bond energies [33].

Inspection of the values for $\Delta E_{\text{d-t}}$(Fe) and $\Delta E_{\text{d-t}}(O_2)$ presented above allows a rationalization of the variety of optimized geometries presented in Table II. For instance, the near coincidence between the geometries obtained with basis sets I (STO-3G for nitrogen, 6-31G for oxygen) and IV [6-31G(d) for nitrogen, 6-31+G for oxygen] can be readily explained because of the compensation between changes in the values of $\Delta E_{\text{d-t}}$(Fe) and $\Delta E_{\text{d-t}}(O_2)$. $\Delta E_{\text{d-t}}$(Fe) is 21.8 kcal/mol smaller (123.7 vs. 145.5) in the case of basis set I, while $\Delta E_{\text{d-t}}(O_2)$ is 25.3 kcal/mol larger (−0.7 vs. −26.0) for this same basis set. The two basis sets that have been discussed in more detail throughout the article, I and II, represent in fact near extreme cases, because the use of the STO-3G description for nitrogen in I gives the maximum stability to the Fe^{III} state, while the use of the 6-31G(d) description for oxygen in II represents the most favorable case for neutral dioxygen. The most accurate result, obtained with basis set VII, is finally an intermediate situation between those obtained with I and II.

Validation of the Computational Method

These results might be put into question by some of the assumptions implicit in the computational method applied. These possible sources of error are analyzed in this section. The first aspect concerns the strong simplification of breaking the conjugation and symmetry of the porphyrin ring in our QM/MM partition. We have

performed a set of calculations with the full porphine ring in order to check the possible differences, especially the energies. We have carried out single point pure QM calculations at Becke3LYP level for all four species involved in the thermodynamic cycle shown in Figure 4, both for basis sets I and II. Results are shown in Table III together with the IMOMM calculated values. The basis set effect on these complexes is reflected on the key $\Delta E_{o\text{-}r}$ value, that makes reference to the relative stabilities of $Fe^{(II)}(P)(O_2)$ and $Fe^{(III)}(P)(O_2^-)$. The pure QM values are -10.9 kcal/mol for basis set I and $+9.3$ kcal/mol for basis set II, to be compared with the IMOMM results (-12.6 and $+10.7$ kcal/mol, respectively). Also in the pure QM calculations, the main factor in this difference arise from the $\Delta E_{d\text{-}t}$ term ($+122.3$ kcal/mol for basis set I and $+146.3$ kcal/mol for basis set II). Although IMOMM and pure QM values are sightly different, the trends are the same, and the same reasoning is valid also for the pure quantum mechanics results.

A second point to be clarified is whether the O_2^- fragment in $Fe(P)(H_2O)(O_2^-)$ complex is a superoxo ligand or not. If it were not, the consideration of gas phase O_2^- in the discussion would not be valid. One possible way to check this point is to compare the improvement in the energies associated with the next reactions on improving the oxygen basis set with diffuse functions:

$$O_2 \rightarrow O_2^-, \qquad \text{(a)}$$

$$Fe^{(II)}(P) + O_2 \rightarrow Fe^{(III)}(P)(O_2^-). \qquad \text{(b)}$$

If the O_2^- fragment in $Fe(P)(H_2O)(O_2^-)$ is a real superoxo ligand, then, the energy improvement associated with the basis set improvement will be the same for both reactions. We have performed calculations using basis sets II and VII on frozen geometries to check this point. These basis sets only differ on the oxygen description: 6-31g(d) in basis set II and 6-31+g(d) in basis set VII. We found the energy improvement to be almost the same, with values of 27.1 kcal/mol for reaction (a) and 23.4 kcal/mol for reaction (b). Then we conclude that the O_2^- fragment in $Fe(P)(H_2O)(O_2^-)$ is a superoxo ligand.

Concluding Remarks

The heavy dependence of the optimized geometry of the $Fe(P)(H_2O)(O_2)$ system on the basis set, with changes in the Fe—O distance of up to 0.7 Å, is related to the qualitatively different electronic description provided by the different basis sets. When the electronic distribution corresponds to a $Fe^{II}(P)$—O_2 description, the oxygen is weakly bound to the iron atom, and the closest Fe—O distance is above 2.7 Å. In contrast, when the description is $Fe^{III}(P)^+$—O_2^-, the bond is much stronger, and the Fe—O distance is in the range of 2.2–2.3 Å. The largest basis set, providing in principle the most accurate result, somehow are brings intermediate situation, with a Fe—O distance of 2.421 Å. The accurate prediction of the geometry for this system requires therefore a quite large basis set.

The dependence of the Fe—O distance on the basis set is, however, not directly related to the description of the interaction between the Fe(P) and O_2 fragments. In fact, the interaction energies between the two fragments computed with frozen geometries changes little, as does the basis set superposition error. The observed sensibility with respect to the basis set of the optimized geometries of heme-dioxygen systems is therefore not necessarily general. For instance, the difference between the Fe^{III} and the Fe^{II} electronic states will probably be very much affected by the eventual presence of an additional coordination ligand. In any case, the results presented in this article indicate that a lot of care must be exerted in the choice of basis set for calculations on this type of system.

ACKNOWLEDGMENTS

Financial support from the Spanish DGESIC through Project No. PB98-0916-CO2-01 and from the Catalan DGR through Project 1999SGR00089 is acknowledged. Thanks are due to the CESCA/CEPBA Computer Center for computer time.

References

1. Stryer, L. Biochemistry, 4th ed; Freeman: New York, 1995.
2. Sono, M.; Roach, M. P.; Coulter, E. D.; Dawson, J. H. Chem Rev 1996, 96, 2841.
3. Momenteau, M.; Reed, C. A. Chem Rev 1994, 94, 659.
4. Lee, J.; Hunt, J. A.; Groves, J. T. J Am Chem Soc 1998, 120, 7493.
5. Sisemore, M. F.; Burstyn, J. N.; Valentine, J. S. Angew Chem Int Ed Engl 1996, 35, 206.
6. Song, R.; Sorokin, A.; Bernadou, J.; Meunier, B. J Org Chem 1997, 62, 673.
7. Dorovska-Taran, V.; Posthumus, M. A.; Boeren, S.; Boersma, M. G.; Teunis, C. J.; Rietjens, I. M. C. M.; Veeger, C. Eur J Biochem 1998, 253, 659.
8. Rohmer, M.-M.; Dedieu, A.; Veillard, A. Chem Phys 1983, 77, 449.
9. Yamamoto, S.; Kashiwagi, H. Chem Phys Lett 1993, 205, 306.

10. Vangberg, T.; Bocian, D. F.; Ghosh, A. J Biol Inorg Chem 1997, 2, 526.
11. Bersuker, I. B.; Leong, M. K.; Boggs, J. E.; Pearlman, R. S. Int J Quantum Chem 1997, 63, 1051.
12. Rovira, C.; Kunc, K.; Hutter, J.; Ballone, P.; Parrinello, M. J Phys Chem A 1997, 101, 8914.
13. Rovira, C.; Ballone, P.; Parrinello, M. Chem Phys Lett 1997, 271, 247.
14. Rovira, C.; Parrinello, M. Chem Eur J 1999, 5, 250.
15. Rovira, C.; Carloni, P.; Parrinello, M. J Phys Chem B 1999, 103, 9387.
16. Kuramochi, H.; Noodleman, L.; Case, D. A. J Am Chem Soc 1997, 119, 11442.
17. Maseras, F. New J Chem 1998, 22, 327.
18. Harris, D. L.; Loew, G. H. J Am Chem Soc 1998, 120, 8941.
19. Spiro, T. G.; Kozlowski, P. M. J Am Chem Soc 1998, 120, 4524.
20. Sigfridsson, E.; Ryde, U. J Biol Inorg Chem 1999, 4, 99.
21. Siegbahn, P. E. M.; Blomberg, M. R. A. Chem Rev 2000, 100, 421.
22. Blomberg, M. R. A.; Siegbahn, P. E. M. J Am Chem Soc 2000, 122, 12848.
23. Ogliaro, F.; Cohen, S.; Filatov, M.; Harris, N.; Shaik, S. Angew Chem Int Ed 2000, 39, 3851.
24. Ogliaro, F.; Cohen, S.; de Visser, S. P.; Shaik, S. J Am Chem Soc 2000, 122, 12892.
25. Maréchal, J.-D.; Barea, G.; Maseras, F.; Lledós, A.; Mouawad, L.; Pérahia, D. J Comput Chem 2000, 21, 282.
26. Maseras, F.; Morokuma, K. J Comput Chem 1995, 16, 1170.
27. Maseras, F. Top Organomet Chem 1999, 4, 165.
28. Frisch, M. J.; Trucks, G. W.; Schlegel, H. B.; Gill, P. M. W.; Johnson, B. G.; Wong, M. W.; Foresman, J. B.; Robb, M. A.; Head-Gordon, M.; Replogle, E. S.; Gomperts, R.; Andres, J. L.; Raghavachari, K.; Binkley, J. S.; Gonzalez, C.; Martin, R. L.; Fox, D. J.; Defrees, D. J.; Baker, J.; Stewart, J. J. P.; Pople, J. A. Gaussian 92/DFT; Gaussian, Inc.: Pittsburgh, PA, 1993.
29. Allinger, N. L. mm3(92); QCPE: Bloomington, IN, 1992.
30. Stephens, P. J.; Devlin, F. J.; Chabalowski, C. F.; Frisch, M. J. J Phys Chem 1994, 98, 11623.
31. Allinger, N. L.; Yuh, Y. H.; Lii, J. H. J Am Chem Soc 1989, 111, 8551.
32. Rohmer, M.-M. in Quantum Chemistry: The Challenge of Transition Metals and Coordination Chemistry; Veillard, A., Ed.; NATO ASI Series C: Mathematical and Physical Sciences; Reidel: Holland, 1986; Vol. 176, p. 377.
33. Partridge, H.; Bauschlicher, C. W.; Sodupe, M.; Langhoff, S. R. Chem Phys Lett 1992, 195, 200.

VI

Theoretical Study of the Reaction Mechanism of Epoxidation of Alkenes with Iodosylbenzene

Guada Barea, Feliu Maseras, and Agustí Lledós

Unitat de Química Física, Departament de Química, Universitat Autònoma de Barcelona, 08193 Bellaterra, Barcelona, Catalonia, Spain.

Sotmès per a la seva publicació al *New Journal of Chemistry*

Theoretical study of the reaction mechanism of the uncatalyzed epoxidation of alkenes by iodosylbenzene

GUADA BAREA, FELIU MASERAS, AGUSTÍ LLEDÓS
Unitat de Química Física, Edifici C.n, Universitat Autònoma de Barcelona, 08193 Bellaterra, Catalonia, Spain.

ABSTRACT: The origin of the barrier for the uncatalyzed epoxidation of alkenes by iodosylbenzene is examined from a computational point of view. The reaction of a monomeric unit with ethylene presents a very low barrier, in disagreement with experimental data indicating the requirement of a catalyst. The polymeric structure of iodosylbenzene is then analyzed, and the importance of the presence of a terminal hydration water in its linear structure confirmed. The reaction of a model dimer with ethylene is shown to have a high barrier in good agreement with experiment. Implications of this result with respect to the nature of the catalytic mechanism are briefly discussed.

Introduction

Olefin epoxidation is by itself a reaction of industrial impact because of the large-scale need for propylene oxide [1]. Although the most commonly applied method is the chlorohydrin process, where the initial attack to the alkene double bond is carried out by a chlorine substituent, the formally simplest approach, direct transfer of one oxygen atom to the alkene is appealing because of the environmental problems created by the chlorohydrin process. The direct transfer method is furthermore a simple example of the oxygen transfer reactions taking place in a number of biological processes, like those in monooxygenase enzymes[2]. Despite its formal simplicity, the detailed mechanisms of these oxygen transfer processes are complex, and they are the subject of intense research both from experimental and theoretical approaches.

There are a variety of experimental systems capable of carrying out an oxygen transfer to an alkene double bond to produce and epoxide. In a number of them, the oxygen added to the olefin comes from a peroxo group [3], either in the form of an organic peroxide [3,4], or coordinated to a transition metal [3,5]. The essential mechanistic features of these processes have been clarified with the help of high-level ab initio computational studies, both in the case of organic peroxides [6,7,8], and of transition metal peroxo complexes [9,10].

In contrast, other experimental systems [11-15] do not use peroxo groups as oxygen source, but other donors like iodosylbenzene or sodium hypochlorite. In these cases, the reaction is almost invariably catalyzed by a transition metal complex. Characteristic examples are

the metal porphyrin systems[11,12], and complexes with salen ligands [13]. These processes take place often through oxo intermediates (**A** in Scheme 1), where the oxygen atom is separated from the donor and attached through a double bond to the metal center. Further support to the intermediacy of oxo species is supplied by the fact that these compounds have been isolated in a number of cases [16]. Consequently, considerable theoretical effort is being invested in the clarification of the part of the mechanism going from the oxo intermediate to the epoxide product [17-19].

Scheme 1

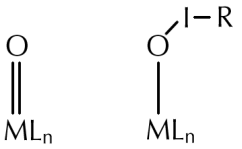

However, there are experimental indications that these reactions of oxygen transfer do not necessarily go in all cases through an oxo intermediate. Koola and Kochi [20] reported already in 1987 the presence of two different mechanisms in olefin epoxidation by salen complexes depending on the nature of the oxygen source. Nam and Valentine [21] confirmed through isotope labeling experiments the presence of these two different mechanisms. They furthermore observed that when the oxygen comes from a peroxide, or a peroxyacid, the oxo intermediate **A** is formed; but that when iodosylbenzene is used there is no oxo complex, and the ethylene is postulated to react directly with a metal-iodosylbenzene complex (**B** in Scheme 1), where the oxygen is bound through single bonds to both the metal center and the iodine atom. Caradonna and co-workers have found a similar duality of mechanisms [22] for the case of bimetallic complexes modeling monoxygenases.

The presence of a catalytic mechanism without oxo complexes is associated in all the reported cases to the use of iodosylbenzene as oxygen donor. Iodosylbenzene is one of the most commonly used reactants for oxygen donation [23]. It has been already suggested that iodosylbenzene is a polymeric solid that operates as a heterogeneous catalyst [24], and that the role of the catalyst is to solubilize it as a monomeric form. In any case, its reaction mechanism for epoxidation reactions has not been subject yet of theoretical analysis. To our knowledge, the only study on related hypervalent iodine compounds was carried out at semiempirical level on $PhIF_2$ and $PhICl_2$ [25].

In this article we analyze from a theoretical point of view the reaction mechanism of the uncatalyzed epoxidation of alkenes with iodosylbenzene. The characterization of this uncatalyzed mechanism will hopefully help the understanding of the role of the catalyst, and thus of the reaction mechanism for the catalyzed process.

Computational Model

In this section we examine the computational model required for a sufficiently accurate description of the reaction mechanism. Three different parameters are considered: (i) the need to introduce the full aromatic ring of iodosylbenzene, (ii) the computational method, and (iii) the basis set. The importance of each of these factors is evaluated through its effect in the exothermicity of the transfer of one oxygen atom from a monomeric iodosyl molecule to and ethylene to yield the corresponding epoxide.

Scheme 2

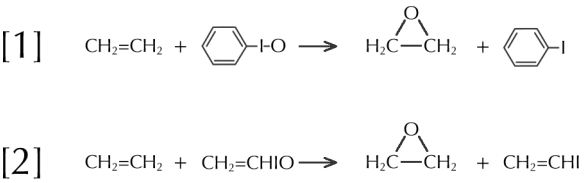

The presence of the phenyl ring increases significantly the size of the system, and hence the computational effort required for its study, and computational cost can be critical when considering polymeric forms of the oxygen donor. On the other hand, the presence of phenyl ring should not be expected to have a very important effect on the key strength of the I-O bond. This effect should be mostly through double bond conjugation, and this aspect could be at least approximately described by the use of the much smaller vinyl group. Thus, we considered modeling the iodososylbenzene molecule (depicted in Equation 1, Scheme 2) by iodosylethylene (Equation 2, Scheme 2).The exothermicity of both reactions was computed through full geometry optimizations of reactants and products with two different computational schemes, B3LYP/I and MP2/I, and the results are shown

Table 1. Exothermicity (kcal/mol) of the reactions between ethylene and the two different iodosyl molecules considered with different methods and basis sets.

	B3LYP/I// B3LYP/I	B3LYP/II// B3LYP/I	MP2/I// MP2/I	MP2/II// MP2/I	CCSD(T)/I //B3LYP/I
Reac. 1	-65.3	-	-70.6	-	-
Reac. 2	-65.6	-63.2	-70.8	-72.4	-67.9

in Table 1. It is clear from the table that iodosylethylene constitutes and excellent computational model for idosylbenzene, with very small changes in the exothermicity of 0.3 kcal/mol at the B3LYP level and of 0.2 kcal/mol at the MP2 level.

A second aspect considered was the computational description. Three different methods were considered for reaction 2: B3LYP, MP2 and CCSD(T). B3LYP and MP2 constitute similar cost representatives of the two major theoretical approaches available: density functional theory and Hartree-Fock based methods, respectively. CCSD(T) is a much more accurate and computationally demanding approach, which is used in this case as a benchmark for the quality of the other two methods. Results are summarized in Table 1. Notation is the usual one, with the basis set separated from the method by a single slash, and the geometry optimization method separated from the energy calculation method by double slashes. While full geometry optimizations were carried out for B3LYP and MP2, CCSD(T) calculations consisted of single-point calculations on the frozen B3LYP geometries. Results are quite similar for the three computational methods. The difference between the B3LYP/I//B3LYP/I and MP2/I//MP2/I is only 5.2 kcal/mol. This difference, which may be too large for other processes, is a small percentage of the total exothermicity. Furthermore, a qualitatively accurate description will be probably sufficient, because the uncatalyzed reaction which is going to be computed should after all have a high barrier. The most accurate CCSD(T) value lies between the B3LYP and MP2 values. We have decided to use the B3LYP method in the calculations because of its more modest requirements in terms of disk space.

The third aspect that has been considered is the basis set. Because of this, the energy difference obtained with basis set I has been recomputed with the significantly more extended basis set II on frozen geometries, at both the B3LYP and MP2 levels. The effect of the basis set is in the range of 2 kcal/mol in both cases. Therefore, we conclude that basis set I is sufficiently accurate, and will be used in the calculations that follow.

After the tests presented in this section, and summarized in Table 1, all calculations in the rest of the article are carried out with the iodosylethylene model, with the B3LYP method and basis set I.

Monomeric System and its Reaction Profile

The first system we analyze is that presented in Equation 2, the direct reaction between the iodosyl compound and ethylene. This system has been already discussed in the previous section. It will suffice here to say that its B3LYP/I exothermicity, corrected with zero point energy, is 62.8 kcal/mol.

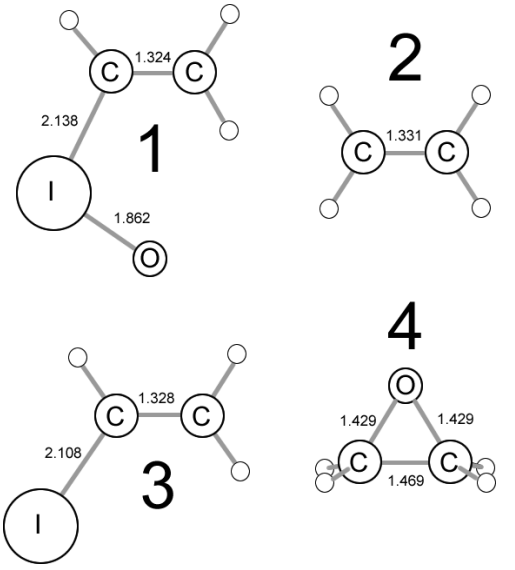

Figure 1. Optimized B3LYP geometries (distances in Å) for iodosylethylene (**1**), ethylene (**2**), iodoethylene (**3**) and ethylene epoxide (**4**).

The optimized geometries of reactants (iodosylethylene, **1**; ethylene, **2**) and products (iodoethylene, **3**; ethylene epoxide, **4**) are presented in Figure 1. The computed bond distances are in all cases reasonable. The C-C distance corresponds to a double bond (between 1.324 and 1.331 Å) in compounds **1** to **3**, while it corresponds to the triangular epoxide arrangement (1.469 Å) in compound **4**. The computed values involving iodine, less known, are in acceptable agreement, taking into account chemical differences, with computed values [26] for iodomethane (C-I, 2.162 Å), and iodosylmethane (C-I, 2.151 Å; I-O, 1.864 Å).

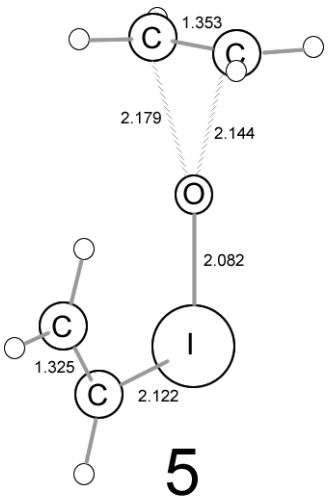

Figure 2. Optimized B3LYP geometries (distances in Å) for the transition state (**5**) of the reaction between monomeric iodosylbenzene and ethylene.

The transition state **5** for the reaction was also computed. Its geometry is presented in Figure 2. The geometry is much more similar to reactants than to products, as can be seen in the epoxide C-C distance of 1.353 Å (to be compared with 1.331 Å in **2** and 1.469 Å in **4**), in agreement with the large exothermicity of the reaction. The energy of the transition state happens to be only 8.3 kcal/mol above that of the reactants. This value was quite unexpected because it would indicate a fast reaction at room temperature. If this were the reaction barrier, there would be no need for catalyst! In fact, this computed value for the reaction of ethylene with monomeric iodosylbenzene computed here is *ca* half the computed value for the reaction of ethylene with peroxyformic acid [7], a reaction that proceeds without catalyst.

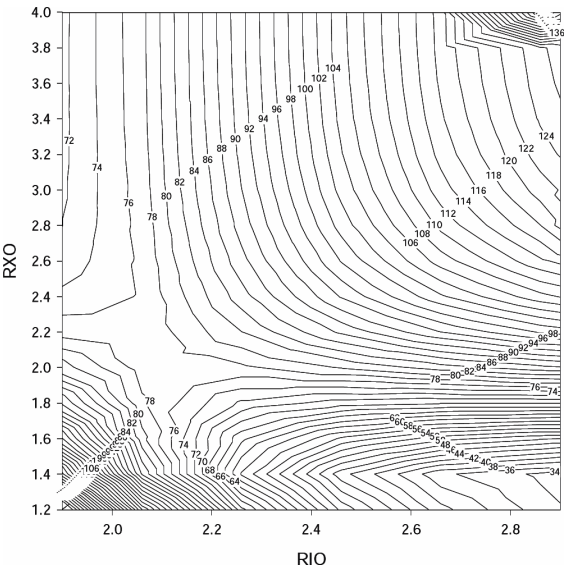

Figure 3. Energy surface for the interaction between frozen iodosylethylene and ethylene as a function of the RIO (I-O) and RXO (O-midpoint of ethylene C-C) distances, in Å. Energies (in kcal/mol) are relative to the energy of ethylene epoxid.

The unexpected presence of such a low energy transition state prompted us to further analyze the reaction path to ensure the absence of some unexpected intermediate or the presence of a higher energy transition state in the path from reactants to products. This study was carried out through the computation of the potential energy surface presented in Figure 3. This surface was obtained by assuming an approach of iodosylethylene to ethylene with the O-I bond perpendicular to the center of the epoxide C-C bond. Single-point calculations were carried out with a variety of values for the I-O and O-(midpoint of ethylene C-C) distances. It can be seen from the surface that there is a clear low energy path connecting the reactants, in the upper left part, with the products, in the lower right part. The values for exothermicity and energy barrier emerging from the graphic are similar, but not exactly identical, to those presented above because of the freezing of coordinates applied in the calculation of the energy surface.

Structure of the Polymeric System

The fact that calculations of the monomeric iodosylethylene system predict a low activation barrier, in poor agreement with experimental data, prompted us to examine the behavior of polymeric units. As mentioned in the introduction, iodosylbenzene is known to be a polymeric solid of low solubility [23,24]. The detailed structure is however not known with precision because of the lack of large crystals to be analyzed by X-ray diffraction.

Scheme 3

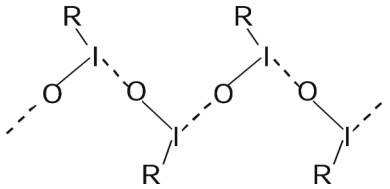

A combination of X-ray powder diffraction and EXAFS techniques [27] indicated the solid structure indicated in Scheme 3 for iodosylbenzene, a linear polymeric, asymmetrically bridged chain structure, where the iodosyl I-O units of different molecules are bound to each other in what has been labeled as secondary bonds [24]. Experimental bond distances are not very accurate because of the lack of large crystals, but the I-O contact between two units of the chain was estimated to be 2.377 Å, while the best estimation for the I-O intramolecular distance was 2.04 Å (corresponding actually to the average between the I-O and I-C distances) [27].

Our attempts to compute short polymeric units of the type $(R\text{-}I\text{-}O)_2$ or $(R\text{-}I\text{-}O)_3$ yielded unsatisfactory results. The geometry optimization produced in practice separation of the system in its monomeric units, which were bound to each other only through weak van der Waals interactions. Things were very different when we added one hydration water to our system, having structures of the form $HO\text{-}(RIO)_n\text{-}H$. In this type of structure, the hydration water is divided in two pieces: the hydroxyl group goes to one end of the chain and it is attached to a iodine; while the remaining hydrogen goes to the other end, and it is attached to an oxygen. This type of arrangement has been suggested from experimental data on aqueous solutions of iodosyl species [28]. When we introduced the hydration water in our calculation of the dimeric $HO\text{-}(R\text{-}I\text{-}O)_2\text{-}H$ system, we obtained structure **6**, shown in Figure 4.

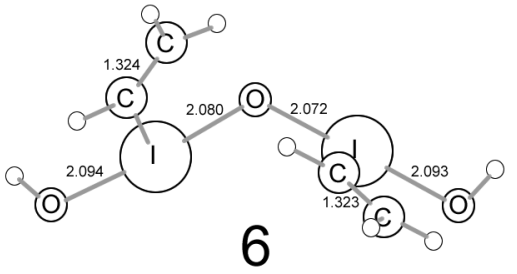

Figure 4. Optimized B3LYP geometry (distances in Å) for the dimeric system (**6**)

Structure **6** has a strong interaction between both monomers, which in fact practically lose their identity. The central oxygen atom shows practically identical bond distances to both iodine atoms (2.072 and 2.080 Å). The terminal hydroxyl groups are also in a very symmetric arrangement with respect to the iodine atoms (I-O bond distances of 2.093 and 2.094 Å). The substantial change in the computed structure of the dimer upon addition of the hydration water gives strong support to the experimental suggestions of its importance [24,28].

The thermodynamic stability of **6** with respect to the separate fragments can be evaluated through the exothermicity of the following reaction:

$$2\ H_2C{=}CHIO + H_2O \ \text{¢}\ HO\text{-}(H_2C{=}CHIO)_2\text{-}H$$

The resulting exothermicity is 41.3 kcal/mol, further confirming that polymeric chains must be completed by a hydration water at its ends.

Agreement between our computed geometry and experimental data is however not perfect. The interaction in our structure is so strong that it becomes more symmetrical in the I-O bond distances (all values between 2.05 and 2.10 Å) than the experimental EXAFS data (two different values of 2.377 and *ca*. 2.05 Å) [27]. We do not consider this discrepancy to be critical, since it is probably related to the fact that we are computing only a 2-member chain. The asymmetry in the experimental study is likely related to the existence of much longer chains, where the symmetrizing effect of the hydration water is probably debilitated throughout this chain. Furthermore, we think that our dimeric system may be a good model of short polymeric units that may dissolve from the solid polymer and act as the reactant for the epoxidation reaction.

The comparison of structure **6** with the geometry of

the monomer **1** (Figure 1) shows that the I-O distance is noticeably longer by 0.2 Å (*ca* 2.07 vs. 1.862 Å) in the dimeric structure, while the I-C distance is slightly shorter by 0.01 Å (*ca* 2.125 vs. 2.138 Å).

Reaction of the Dimeric System

The interaction of the dimer **6** with ethylene was studied. Three different stationary points were located in the potential energy hypersurface. All of them have been characterized through calculation of the second derivatives. Two of them correspond to local minima (zero imaginary frequencies) and the remaining one is the transition state connecting them (one imaginary frequency).

The first geometry computed for this system, labeled as **7**, is an adduct corresponding to the initial approach of ethylene to **6**. The distance between the fragments is still large, with the ethylene carbon closer to the central oxygen of the dimer still 3.511 Å away from it. Consequently, the geometry of the dimer part in **7** is very similar to that in **6**, and the energy of **7** is only slightly (0.2 kcal/mol) below that of the separate reactants.

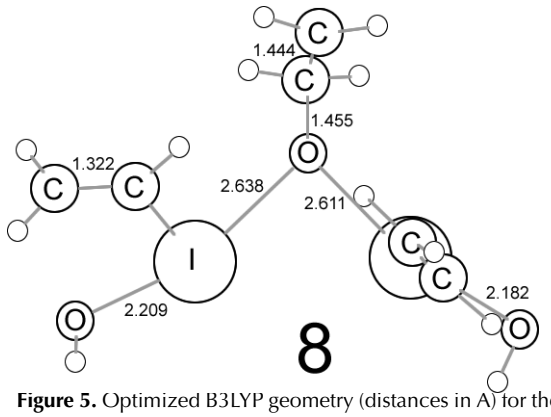

Figure 5. Optimized B3LYP geometry (distances in A) for the transition state **8**.

The second geometry computed for this system is the transition state **8**, shown in Figure 5. **8** has one single imaginary frequency, with a value of 339i cm^{-1}. Its connectivity to reactant **7** and product **9**, presented below, was confirmed through intrinsic reaction coordinate calculations [29]. The most remarkable characteristic of **8** is its energy, which is 48.5 kcal/mol above the reactants. This high value is in agreement with the practical absence of uncatalyzed reaction. The breaking of the polymeric chain is therefore the origin of the large energy barrier for this reaction, and the main role of catalysts will be therefore the breaking of the chain.

There are several aspects in the geometry of **8** that merit discussion. The breaking of the two oxygen-iodine bonds takes place in a synchronous manner. The oxygen atom being transferred is still symmetrically bound to the two iodine atoms to the which it was attached in reactant **7**. The I-O distance increases much when going from the reactant (*ca* 2.1 Å) to the transition state (*ca* 2.6 Å). This means essentially that the oxygen must be completely separated from the two iodine atoms before completing the formation of the epoxide. This is consistent with the high barrier: old bonds are completely broken before the new ones are formed. The formation of the two oxygen-carbon bonds is in contrast completely asynchronous. While one of the ethylene carbons is already practically at the epoxide distance (1.445 Å), the other is still very far from the oxygen (2.054 Å). The computed asymmetry in the transition state with respect to the C-O bonds corresponds probably to chemical reality because the B3LYP method applied is not affected by the bias of the MP2 method favoring asymmetric structures reported for epoxidation reactions with other agents [30]. It is worth noticing that calculations with the same computational method indicate a synchronous formation of both C-O bonds in the permitted reaction of unsubstituted alkenes with peroxyformic acid [7].

The third structure optimized for this system is product **9**. As mentioned above, this structure has been shown to be related to transition state **8** through an IRC calculation. **9** can be seen as composed of three nearly independent fragments: ethylene epoxide and two independent H_2C=CH(IOH) units. The identification of the reaction product, ethylene epoxide, is clear from a variety of geometrical parameters. The oxygen has beencompletely transferred to the epoxide, with C-O distances of 1.434 Å and 1.446 Å; and taken away from the dimer, the closer distances to the other two fragments being an O-H distance of 2.392 Å and a I-O distance of 3.137 Å, both of them clearly non-bonding. The energy of this product is 1.21 kcal/mol above that of the separated reactants.

The fact that the energy of this product is above that of the reactants can seem surprising, but it can be easily corrected by looking at the rather peculiar nature of the product. There are two H_2C=CH(IOH) fragments, which in principle should not be expected to be very stable. These molecules are probably going to evolve in solution to produce more stable products. In particular, we have considered the thermodynamics of the reaction:

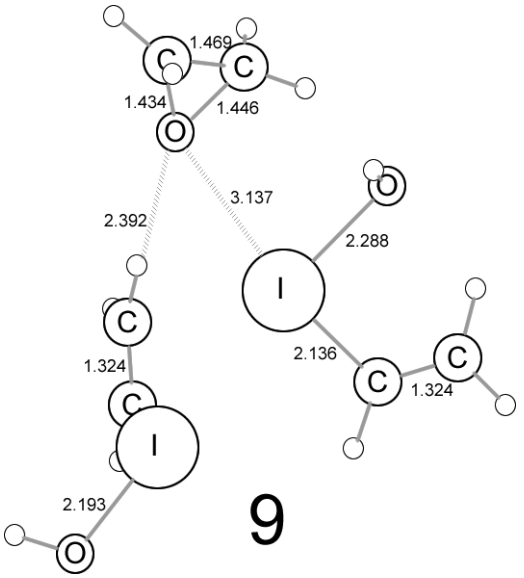

Figure 6. Optimized B3LYP geometry (distances in Å) for the product **9**.

2 H_2C=CH(IOH) ¢ H_2C=CHI + H_2C=CH(IO) + H_2O

This reaction is exothermic by 27.9 kcal/mol. The epoxidation reaction with a dimeric iodosylethylene is therefore quite exothermic, but with a high reaction barrier of *ca* 50 kcal/mol.

Discussion

Our calculations indicate that the monomeric form of iodosylethylene would be able to carry out the epoxidation without any barrier. On the other hand, the dimeric form, which constitutes a more realistic model of the experimental polymeric compound, yields a barrier near 50 kcal/mol. It is therefore clear that the barrier is intimately related to the existence of the polymer. Therefore, the main role of any catalyst will be to break this polymeric structure.

This result provides a simple explanation to the presence of two different mechanisms, depending on the particular catalyst, in the epoxidation of olefins by iodosylbenzene [20,21,15]. The difference between these two mechanisms, described in the introduction and depicted in Scheme 1, is the nature of the reaction intermediate, which can be an oxo compound where the oxygen is completely separated from iodine **A**, or it can contain still a iodine attached to the oxygen **B**. The existence of these intermediates corresponds to a stage where the polymeric structure, with the oxygen attached to two iodine atoms is already broken. Because of this, the particular nature of the intermediate, **A** or **B**, is not as critical as its existence, and the reaction can take place through quite different intermediates. The existence of «monomeric» soluble derivatives of iodosylarene [24], stabilized by intramolecular interactions, looks therefore as a promising way to convert these species as oxygen donors without the need for catalysts. The behavior described in this work is likely characteristic of iodosylbenzene, and cannot be directly extrapolated to other oxygen donors, where the abstraction of oxygen from the donor may be concerted with its transfer to the epoxide.

Computational Details

All calculations were carried out with the Gaussian 98 program [31]. Although most calculations were carried out with the density functional B3LYP, calibration calculations presented in the section dealing with the computational method also used the MP2 and CCSD(T) methods.Two different basis sets were used. Basis set I was valence double-ζ with a polarization shell in all atoms except hydrogen. In particular, the iodine was described by a pseudopotential and the associated LANL2DZ basis set [32] supplemented with a polarization d shell [33], while the 6-31G(d) basis was used for C, O, H [34,35]. Basis set II, which calibration calculations presented in the text proved as unnecessarily expensive, was valence triple-ζ and included polarization shells in all atoms, including hydrogens. In the case of iodine this quality was accomplished by splitting the primitives in the LANL2DZ basis set commented above, while the 6-311G(d,p) basis [36] was used for all other atoms.Except in the calibration calculations, the nature of all the computed stationary points as local minima or transition states has been confirmed through analytical second derivative calculations, and the energies presented are internal energies including zero point corrections. Intrinsic reaction coordinate calculations were carried out to confirm the connectivity between transition state **8** and local minima **7** and **9**.

Concluding Remarks

Theoretical B3LYP calculations on a iodosylethylene model allow to understand the main features of the reactivity of iodosylbenzene towards the uncatalyzed epoxidation of olefins, and provide significant clues on the mechanism of catalysis. A monomeric iodosylbenzene would produce the epoxidation reaction with a very low barrier, and the experimentally observed high barrier appears only when the polymeric nature of the iodosyl species is taken into account. This computational study has also allowed a better understanding of the polymeric structure, emphasizing the important role of the presence of a hydration water in the chain ends.

The origin of the barrier for the uncatalyzed epoxidation with iodosylbenzene is precisely the extraction of oxygen from the strongly bound polymer. Because of this, seemingly different catalysts able to break the polymer but forming different types of intermediates afterwards are efficient in this process.

Acknowledgment. Financial support is acknowledged from the Spanish DGES (project No. PB98-0916-C02-01) and the Catalan DURSI (project No. 1999 SGR00089). FM thanks also the support of DURSI.

References

[1] Weissermel, K.; Arpe, H. -J. Industrial Organic Chemsitry, 3rd Ed.; Wiley-VCH: New York, 1997.
[2] Lippard, S. J.; Berg, J. M. Bioinorganic Chemistry; University Science Books: Mill Valley, CA, 1994.
[3] (a) Adam, W.; Mitchell, C. M.; Saha-Möller, C. R. *J. Org. Chem.* **1999**, *64*, 3699. (b) Adam, W.; Wirth, T. *Acc. Chem. Res.* **1999**, *32*, 703.
[4] Adam, W.; Nestler, B. *Tetrahedron Letters* **1993**, *34*, 611.
[5] (a) Romão, C. C.; Kühn, F. E.; Herrmann, W. A. *Chem. Rev.* **1997**, *97*, 3197. (b) Wahl, G.; Kleinhenz, D.; Schorm, A.; Sundermeyer, J.; Stowasswer, R.; Rummey, C.; Bringmann, G.; Fickert, C.; Kiefer, W. *Chem. Eur. J.* **1999**, *5*, 3237.
[6] Houk, K. N.; condroski, K. R.; Pryor, W. A. *J. Am. Chem. Soc.* **1996**, *118*. 13002.
[7] (a) Bach, R. D.; Estévez, C. M.; Winter, J. E.; Glukhovtsev, M. N. *J. Am. Chem. Soc.* **1998**, *120*, 680. (b) Bach, R: D.; Glukhovtsev, M. N.; GOnzalez, C. *J. Am. Chem. Soc.* **1998**, *120*, 9902.
[8] Adam, W.; Bach, R. D.; Dmitrenko, O.; Saha-Möller, C. R. *J. Org. Chem.* **2000**, *65*, 6715.
[9] (a) Gisdakis, P.; Antonczak, S.; Köstlmeier, S.; Herrmann, W. A.; Rösch, N. *Angew. Chem. Int. Ed. Engl.* **1998**, *37*, 2211. (b) Valentin, C. D.; Gandolfi, R.; Gisdakis, P.; Rösch, N. *J. Am. Chem. Soc.* **2001**, *123*, 2365.
[10] (a) Deubel, D.V.; Sundermeyer, J.; Frenking, G. *Inorg. Chem.* **2000**, *39*, 2314. (b) Deubel, D. V.; Sundermeyer, J.; Frenking, G. *J. Am. Chem. Soc.* **2000**, *122*, 10101.
[11] Groves, J. T.; Myers, R. S. *J. Am. Chem. Soc.* **1983**, *105*, 5791.
[12] (a) Tai, A. F.; Margerum, L. D.; Valentine, J. S. *J. Am. Chem. Soc.* **1986**, *108*, 5006. (b) Nam, W.; Valentine, J. S. *J. Am. Chem. Soc.* **1990**, *112*, 4977. (c) Yang, Y.; Diederich, F.; Valentine, J. S. *J. Am. Chem. Soc.* **1991**, *113*, 7195.
[13] (a) Samsel, E. G.; Srinivasan, K.; Kochi, J. K. *J. Am. Chem. Soc*. **1985**, *107*, 7606. (b) Jacobsen, E. N. In Catalytic Asymmetric Synthesis; Ojima, I. Ed.; VCH: New York, 1993, pp 159. (c) Katsuki, T. *Coord. Chem. Rev.* **1995**, *140*, 189.
[14] Gross, Z.; Ini, S. *J. Org. Chem.* **1997**, *62*, 5514. (b) Gross, Z.; Simkhovich, Galili, N. *J. Chem. Soc., Chem. Commun.* **1999**, 599.
[15] (a) Stassinopoulos, A.; Caradonna, J. P. *J. Am. Chem. Soc.* **1990**, *112*, 7071. (b) Mukerjee, S.; Stassinopoulos, A.; Caradonna, J. P. *J. Am. Chem. Soc.* **1997**, *119*, 8097.
[16] (a) Groves, J. T.; Haushalter, R. C.; Nakamura, M.; Nemo, T. E.; Evans, B. J. *J. Am. Chem. Soc.* **1981**, *103*, 2884. (b) Feichtinger, D.; Plattner, D. A. *Angew. Chem. Int. Ed. Engl.* **1997**, *109*, 1796. (c) Jin, N.; Groves, J. T. *J. Am. Chem. Soc.* **1999**, *121*, 2923.
[17] (a) Norrby, P. -O.; Linde, C.; Åkermark, B. *J. Am. Chem. Soc.* **1995**, *117*, 11035. (b) Linde, D.; Åkermark, B.; Norrby, P. -O.; Svensson, M. *J. Am. Chem. Soc.* **1999**, *121*, 5083.
[18] (a) Cavallo, L.; Jacobsen H. *Angew. Chem. Int. Ed. Engl.* **2000**, *39*, 589. (b) Jacobsen, H.; Cavallo, L. *Chem. Eur. J.* **2001**, *7*, 800.
[19] de Visser, S. P.; Ogliaro, F.; Harris, N.; Shaik, S. *J. Am. Chem. Soc.* **2001**, *123*, 3037.
[20] Koola, J. D.; Kochi, J. K. *J. Org. Chem.* **1987**, *52*, 4545.
[21] Nam, W.; Valentine, J. S. *J. Am. Chem. Soc.* **1993**, *115*, 1772.
[22] Mukerjee, S.; Skogerson, K.; DeGala, S.; Caradonna, J. P. *Inorg. Chim. Acta* **2000**, *297*, 313.
[23] (a) Varvoglis, A. Hypervalent Iodine in Organic Synthesis; Academic Press: San Diego, 1997. (b) Stang, P. J.; Zhdankin, V. V. *Chem. Rev*. **1996**, *96*, 1123.
[24] (a) Macikenas, D.; Skrzypczak-Jankun, W.; Protasiewicz, J. D. *J. Am. Chem. Soc.* **1999**, *121*, 7164. (b) Macikenas, D.; Skrzypczak-Jankun, W.; Protasiewicz, J. D. *Angew. Chem. Int. Ed. Engl.* **2000**, *39*, 2007.
[25] Mylonas, V. E.; Sigalas, P.; Katsoulos, G. A.; Tsipis, C. A.; Varvoglis, A. G. *J. Chem. Soc. Perkin Trans. 2* **1994**, 1691.
[26] Misra, A.; Berry, R. J.; Marshall, P. J. Phys. Chem. A 1997, 101, 7420.
[27] Carmalt, C. J.; Crossley, J. G.; Knight, J. G.; Lightfoot, P.; Martín, A.; Muldowney, M. P.; Norman, N. C.; Orpen, A. G. *J. Chem. Soc., Chem. Commun*. **1994**, 2367.
[28] Richter, H. W.; Cherry, B. R.; Zook, T. D.; Koser, G. F. *J. Am. Chem. Soc.* **1997**, *119*, 9614.

[29] Gonzalez, C.; Schlegel, H. B. *J. Phys. Chem.* **1990**, *94*, 5523.
[30] Bach, R. C.; Glukhovtsev, M. N.; Gonzalez, C.; Marquez, M.; Estévez, C. M.; Baboul, A. G.; Sclegel, H. B. *J. Phys. Chem. A* **1997**, *101*, 6092.
[31] Frisch, M. J.; Trucks, G. W.; Schlegel, H. B.; Scuseria, G. E.; Robb, M. A.; Cheeseman, J. R.; Zakrzewski, V. G.; Montgomery, Jr., J. A.; Stratmann, R.E.; Burant, J. C.; Dapprich, S.; Millam, J. M.; Daniels, A. D.; Kudin, K. N.; Strain, M. C.; Farkas, O.; Tomasi, J.; Barone, V.; Cossi, M.; Cammi, R.; Mennucci, B.; Pomelli, C.; Adamo, C.; Clifford, S.; Ochterski, J.; Petersson, G. A.; Ayala, P. Y.; Cui, Q.; Morokuma, K.; Malick, D. K.; Rabuck, A. D.; Raghavachari, K.; Foresman, J. B.; Cioslowski, J.; Ortiz, J. V.; Stefanov, B. B.; Liu, G.; Liashenko, A.; Piskorz, P.; Komaromi, I.; Gomperts, R.; Martin, R. L.; Fox, D. J.; Keith, T.; Al-Laham, M. A.; Peng, C. Y.; Nanayakkara, A.; Gonzalez, C.; Challacombe, M.; Gill, P. M. W.; Johnson, B.; Chen, W.; Wong, M. W.; Andres, J. L.; Gonzalez, C.; Head-Gordon, M.; Replogle, E. S.; Pople, J. A. Gaussian 98; Gaussian, Inc.: Pittsburgh PA, 1998.
[32] Wadt, W. R.; Hay, P. J. *J. Chem. Phys.* **1985**, *82*, 284.
[33] Höllwarth, A.; Böhme, M.; Dapprich, S.; Ehlers, A. W.; Gobbi, A.; Jonas, V.; Köhler, K. F.; Stegmann, R.; Veldkamp, A.; Frenking, G. Chem. Phys. Letters 1993, 208, 237.
[34] Hehre, W. J.; Ditchfield, R.; Pople, J. A. *J. Chem. Phys.* **1972**, *56*, 2257.
[35] Hariharan, P. C.; pople, J. A. *Theor. Chim. Acta* **1973**, *28*, 213.
[36] Krishnan, R.; BLinkey, J. S.; Seeger, R.; Pople, J. A. *J. Chem. Phys.* **1980**, *72*, 650.

Bibliografia

[1] Greenwood, N. N.; Earnshaw, A. *Chemistry of the Elements*, Pergamon press, Oxford, 1984.

[2] Crabtree, R. H. *The Organometallic Chemistry of the Transition Metals*, 3th ed. Wiley, New York, 2001.

[3] Levine, I. N. *Quantum Chemistry* 5th ed. Prentice-Hall, Inc. Upper Saddle River, New Jersey, 2000.

[4] Szabo, A.; Ostlund, N. S. *Modern Quantum Chemistry* rev. ed. Dover, 1996.

[5] Rappé, A. K.; Casewit, C. J. A *Molecular Mechanics across Chemistry*, Univeristy Science Books, Sausalito: California, 1997.

[6] Schleyer, P. v. R.; Allinger, N. L.; Clark, T.; Gasteiger, J.; Kollman, P. A.; Schaefer, H. F.; Schreiner, P. R. *The encyclopedia of Computational Chemistry*, Wiley, New York, 1998.

[7] Pople, J. A. *Angew. Chem. Int. Ed. Engl*. **1999**, *38*, 1894.

[8] Davidson, E. R. *Chem. Rev*. **2000**, *100*, 351.

[9] Maseras, F.; Lledós, A.; Clot, E.; Eisenstein, O. *Chem. Rev*. **2000**, *100*, 601.

[10] Cundari, T. R. (ed.) *Computational Organometallic Chemistry*, Marcel Dekker, New York, 2000.

[11] Hartree, D. *Proc. Cambridge Phil. Soc*. **1928**, *24*, 89 (b) Hartree, D. *Proc. Cambridge Phil. Soc*. **1928**, *24*, 111. (c) Hartree, D. *Proc. Cambridge Phil. Soc*. **1928**, *24*, 426.

[12] Fock, V. *Physik* **1929**, *61*, 126.

[13] Møller, C.; Plesset, M. S. *Phys Rev*. **1934**, *46*, 618.

[14] Olsen, J.; Yeager, D. L.; Jorgensen, P. *Adv. Chem. Phys*. **1983**, *54*, 1.

[15] Shavitt, I. H. F. Schaefer III Ed. *Methods of Electronic Structure Theory*, Plenum Press, New York, 1977.
[16] Parr, R. G.; Yang, W. *Density Functional Theory of Atoms and Molecules*, Oxford University Press, New York, 1989.
[17] Ziegler, T. *Chem. Rev*. **1991**, *108*, 651.
[18] Thiel, W.; Voityuk, A. *Theor. Chim. Acta* **1992**, *81*, 391.
[19] Dewar, M. J. S.; Jie, C.; Yu, *Tetrahedron* **1993**, *49*, 5003.
[20] Andersson, W. P.; Edwards, W. D.; Zerner, M. C. *Inorg. Chem*. **1986**, *25*, 2728.
[21] Hehre, W. J.; Yu, J.; Klunziguer, P. E. *A Guide to Molecular Mechanics and Molecular Orbital Calculations in Spartan*; Wavefunction Inc., Irvine, California, 1997.
[22] Bosque, R.; Maseras, F. *J. Comput. Chem*. **2000**, *21*, 562.
[23] Hoffman, R. *J. Chem. Phys*. **1963**, *39*, 1397.
[24] Albright, T. A.; Burdett, J. K.; Whangbo, M. H. *Orbital interactions in chemistry*. Wiley, New York, 1985.
[25] Hohenberg, P.; Kohn, W. *Phys. Rev. B* **1964**, *136*, 864.
[26] Allinger, N. L.; Yuh, Y. H.; Lii, J. -H. *J. Am. Chem. Soc*. **1989**, *111*, 8551.
[27] Weiner, S. J.; Kollman, P. A.; Nguyen, D. T.; Case, D. A. *J. Comput. Chem*. **1986**, *7*, 230.
[28] Brooks, B. R.; Bruccoleri, R: E.; Olafson, B. D.; States, D. J.; Swaminathan, J.; Karplus, M. *J. Comput. Chem*. **1983**, *4*, 187.
[29] Comba, P.; Hambley, T. W. A *Molecular Modelling across Chemistry*, University Science Books, Susalito, California, 1997.
[30] Zimmer, M. *Chem. Rev*. **1995**, *95*, 2629.
[31] Rappé, A. K.; Casewit, C. J.; Colwell, K. S.; Goddard, W. A., III; Skiff, W. M. *J. Am. Chem. Soc*. **1992**, *114*, 10024.
[32]Norrby, P.-O. A *Computational Organometallic Chemistry,* Marcel Dekker pàg. 7, 2001.
[33] Bakowies, D.; Thiel, W. *J. Phys. Chem*. **1996**, *100*, 10580.
[34] Thery, V.; Rinaldi, D. Rivail, J.-L.; Maigret, B.; Ferenczy, G.G. *J. Comput. Chem*. **1994**, *15*, 269.
[35] Tuñón, I.; Martins-Costa, M.T.C.; Millot, C.; Ruiz-López, M. F. Rivail, J. -L. *J. Comput. Chem*. **1996**, *17*, 19.
[36] Tuñón, I.; Martins-Costa, M.T.C.; Millot, C.; Ruiz-López, M. F. *J. Chem. Phys*. **1997**, *106*, 3633.
[37] Strnad, M.; Martins-Costa, M.T.C.; Millot, C.; Tuñón, I.; Ruiz-López, M.F.; Rivail, J.-L. *J. Chem. Phys*. **1997**, *106*, 3643.

[38] Field, M.; Bash, A.; Karplus, M. *J. Comput. Chem*. **1990**, *11*, 700.
[39] Singh, U. C.; Kollman, P. A. *J. Comput. Chem*. **1986**, *7*, 718.
[40] Thompson, M. A. *J. Chem. Phys*. **1995**, *99*, 4794.
[41] Eurenius, K. P.; Chatfield, D. C.; Brooks, B: R.; Hodoscek, M. *Int. J. Quantum Chem*. **1996**, *60*, 1189.
[42] Maseras, F.; Morokuma, K. *J. Comput. Chem*. **1995**, *100*, 2573.
[43] Maseras, F. A *Computational Organometallic Chemistry*, Marcel Dekker, New York, 2001, pàg. 159.
[44] Maseras, F. *Top. Organomt. Chem*. **1999**, *4*, 165.
[45] Maseras, F. *Chem. Commun*. **2000**, 1821.
[46] Einstein, F. W. B.; Johnston, V: J.; Ma, A: K.; Pomeroy, R. K. *Organometallics*, **1990**, *9*, 52.
[47] Taft, R: W.; Glick, R. E.; Lewis, I. C.; Fox, I.; Ehrenson, S. *J. Am. Chem. Soc*. **1960**, *82*, 756.
[48] Cotton, J. D.; Miles, E. A. *Inorg. Chim. Acta*, **1990**, *173*, 129.
[49] Onaka, S.; Takagi, S.; Furuta, H.; Kato, Y.; Mizuno, A. *Bull. Chem. Soc. Jpn*. **1990**, *63*, 42.
[50] (a) Taft, R. W. A *Steric Effects in Organic Chemistry*, Newman, M. S. Ed.; Wiley, New York, 1956. (b) MacPhee, J. A.; Panaye, A.; Dubois, J. -E. *Tetrahedron*, **1978**, *34*, 3553. (c) Panaye, A.; Macphee, J. A.; Dubois, J. -E. *Tetrahedron*, **1980**, *36*, 759.
[51] Staskun, B. *J. Org. Chem*. **1981**, *46*, 1643.
[52] Tolman, C. A. *Chem. Rev*. **1977**, *77*, 313.
[53] de Santo, J. T.; Mosbo, J. A.; Storhoff, B. -N.; Bock, P. L. Bloss, R. E. *Inorg. Chem*. **1980**, *19*, 3086.
[54] Brown, T. L. *Inorg. Chem*. **1992**, *31*, 1286.
[55] Gusev, D. G.; Berke, H. *Chem. Ber*. **1996**, *129*, 1143.
[56] Bau, R.; Drabnis, M. H. *Inorg. Chim. Acta* **1997**, *259*, 27.
[57] Sabo-Etienne, S.; Chaudret, B. *Chem. Rev*. **1998**, *98*, 2077.
[58] Esteruelas, M. A.; Oro, L. A. *Chem. Rev*. **1998**, *98*, 577.
[59] Howard, J. A. K.; Keller, P. A.; Vogt, T.; Taylor, A. L.; Dix, N. L.; Spencer, J. L. *Acta Cryst*. **1992**, *B48*, 438.
[60] Loza, M. L.; de Gala, S. R.; Crabtree, R. H. *Inorg. Chem*. **1994**, *33*, 5073.
[61] (a) Dreisch, K.; Andersson, C.; Stalhandske, C. *Polyhedron* **1993**, *12*, 303. (b) Allen, F. H.; Kennard, O. *Chem. Des. Autom. News* **1993**, *8*, 31.
[62] Lippard, S. J.; Berg, J. M. Bioinorganic Chemistry. University Science Books, Mill Valley, California, 1994.
[63] Strayer, L. Biochemistry. Freeman, New York, 1996.

[64] Solomon, E. I. *Chem. Rev*, **1996**, *96*, 2239.
[65] Siegbahn, P. E. M.; Blomberg, M. R. A. *Chem. Rev*. **2000**, *100*, 421.
[66] Perutz, M. F. *Proc. R. Soc. Lond. Ser.* **1980**, *B208*, 135.
[67] Perutz, M. F.; Fermi, G.; Luisi, B.; Shaanan, B.; Liddington, R: C. *Acc. Chem. Res*. **1987**, *20*, 309.
[68] Welinder, K. G. *Curr. Opin. Struct. Biol*. **1992**, *2*, 388.
[69] Sono, M.; Roach, M. P.; Coulter, E. D.; Dawson, J. H. *Chem. Rev*. **1996**, *96*, 2841.
[70] Perutz, M. F. *Science*, **1963**, *140*, 863.
[71] Momenteau, M.; Reed, C. A. *Chem Rev*. **1994**, *94*, 659.
[72] Zerner, M.; Gouterman, M.; Kobayashi, H. *Theoret. Chim. Acta* **1966**, *6*, 363.
[73] Olafson, B: D.; Goddard, W. A. *Proc. Natl. Acad. Sci. USA*, **1977**, *74*, 1315.
[74] Dedieu, A.*Nouv. J. Chim*. **1979**, *3*, 653.
[75] Rohmer, M. -M. *Chem. Phys. Letters* **1985**, *44*, 116.
[76] Saito, M.; Kashiwagi, H. *J. Chem. Phys*. **1985**, *82*, 3716.
[77] Case, D. A.; Huynh, B. H.; Karplus, M. *J. Am. Chem. Soc.* **1979**, *101*, 4433.
[78] (a) Herman, Z. S.; Loew, G. H.; Rohmer, M. -M. *Int. J. Quantum Chem.* **1980**, *QBS7*, 137. (b) Loew, G. H.; Herman, Z. S.; Zerner, M. C. *Int. J. Quantum Chem.* **1980**, *18*, 481. (c) Waleh, A.; Ho, N.; Chantranupong, L.; Loew, G. H. *J. Am. Chem. Soc.* **1989**, *111*, 2767.
[79] Jewsbury, P. Yamamoto, S.; Minato, T.; Saito, M.; Kitagawa, T. *J. Am. Chem. Soc*. **1994**, *116*, 11586.
[80] (a) Yamamoto, S.; Kashiwagi, H. *Chem. Phys. Letters* **1989**, *161*, 85. (b) Yamamoto, S.; Kashiwagi, H. *Chem. Phys. Letters* **1993**, *206*. 306.
[81] Nakatsuji, H.; Hasegawa, J.; Ueda, H.; Hada, M. *Chem Phys. Letters* **1996**, *250*, 379.
[82] Ghosh, A.; Bocian, D. F. *J. Phys. Chem*. **1996**, *100*, 6363.
[83] Vangberg, T.; Bocian, D. F.; Ghosh, A. *J. Biol. Inorg. Chem.* **1997**, *2*, 526.
[84] Spiro, T. G.; Kozlowski, P. M. *J. Am. Chem. Soc.* **1998**, *120*, 4524.
[85] Godbout, N.; Sanders, L. K.; Salzmann, R.; Havlin, R. H.; Wojdeski, M.; Oldfield, E. *J. Am. Chem. Soc.* **1999**, *121*, 3829.
[86] Sigfridsson, E.; Ryde, U. *J. Biol. Inorg. Chem*. **1999**, *4*, 99.
[87] Rovira, C.; Carloni, P.; Parrinello, M. *J. Phys. Chem. B* **1999**, *103*, 7031.
[88] Zakharieva, O.; Grodzicki, M.; Trautwein, A., X.; Veeger, C.; Rietgens, I. M. C. M. *J. Bioinorg. Chem.* **1996**, *1*, 192.
[89] Green, T. *J. Am. Chem. Soc*. **1998**, *120*, 10772.
[90] Loew, G: H.; Harris, D. *Chem. Rev.* **2000**, *100*, 407.

[91] Brooks, B. R.; Bruccoleri, R. E.; Olafson, B. D.; States, D. J.; Swaminathan, J.; Karplus, M. *J. Comput. Chem*. **1983**, *4*, 187.
[92] Kuczera, K.; Kuriyan, J.; karplus, M. *J. Mol. Biol*. **1990**, *213*, 351.
[93] Kozlowski, P. M.; Zgierski, M.; Pulay, M. *Chem. Phys. Letters* **1995**, *247*, 379.
[94] Franzen, S.; Bohn, B.; Poyart, C.; DePillis, G. *J. Biol. Chem.* **1995**, *270*, 1718.
[95] Warshel, A.; Levitt, M. *J. Mol. Biol*. **1976**, *103*, 227.
[96] (a) Gao, J. *Acc. Chem. Res.* **1996**, *29*, 298. (b) Gao, J. *Rev. Comput. Chem*. **1996**, *7*, 119.
[97] Bytheway, I.; Hall, M. B. *Chem. Rev*. **1994**, *94*, 639.
[98] Jameson, G. B.; Rodley, G. A.; Robinson, W. T.; Gagne, R. R.; Reed, C. A.; Collman, J. P. *Inorg. Chem.* **1978**, *17*, 850.
[99] Momenteau, M.; Scheidt, W. R.; Eigenbrot, C. W.; Reed, C. A. *J. Am. Chem. Soc*. **1988**, *110*, 1207.
[100] Li, N. Y.; Su, Z. W.; Coppens, P.; Landrum, J. *J. Am. Chem. Soc*. **1990**, *112*, 7294.
[101] Maréchal, J. -D.; Maseras, F.; Lledós, A.; Pérahia, D.; Mouawad, L. *Chem. Phys. Lett*. **2002**. En premsa.
[102] Dunfort, H. B.; Stillman, J. S. *Coord. Chem. Rev.* **1976**, 19.
[103] Corrall, R. J. M.; Rodman, H. M.; Margolis, J.; Landau, B. L. *J. Biol. Chem.* **1974**, *249*, 3181.
[104] (a) Edwards, S. L.; Xuong, N. H.; Hamlin, R. C.; Kraut, J. *Biochemistry*, **1987**, *26*, 1503. (b) Fulop, V.; Erman, J.; Hajdu, J.; Edwards, S. L. *Structure*, **1994**, *2*, 201.
[105] Poulos T. L.; Kraut, J. *J. Biol. Chem.* **1980**, *225*, 8199.
[106] (a) Selke, M.; Sisemore, M. F.; Valentine, J. S. *J. Am. Chem. Soc.* **1996**, *118*, 2008. (b) Sisemore, M. F.; Selke, M.; Burstyn, J. N.; Valentine, J. S. *Inorg. Chem.* **1997**, *36*, 979. (c) Selke, M.; Valentine, J. S. *J. Am. Chem. Soc*. **1998**, *120*, 2652.
[107] (a) Hartmann, M.; Robert, A.; Duarte, V.; Keppler, B. K.; Meunier, B. *J. Biol. Inorg. Chem*. **1997**, *2*, 427. (b) Balahura, R: J.; Sorokun, A.; Bernadou, J.; Meunier, B. *Inorg. Chem*. **1997**, *36*, 3488. (c) Song, R.; Sorokin, A.; Bernadou, J.; meunier, B. *J. Org. Chem*. **1997**, *62*, 673. (d) Wietzerbin, K.; meunir, B.; Bernadou, J. *Chem. Commun*. **1997**, 2321.
[108] Dunford, H. B. A *Peroxidase in Chemistry and Biology*; Everse, J.; Everse, K. E.; Grsiham, M. B. Eds.; CRC Press, Boca Raton, Florida. 1991; Vol. 2, p.1.
[109] McMurry, T. J.; Groves, J. T. A *Cythocrome P-450, Structure, Mechanism*

and Biochemistry; Ortiz de Montellano, P. R. Ed.; Plenum Press, New York. 1986, p.1.
[110] Holm, R. H. *Chem. Rev*. **1987**, *87*, 1401.
[111] Mlodnika, T. A *Metalloporphyrins in Catalytic Oxidation*; Sheldon, R. A.; Ed.; Marcel Dekker: New York. 1994, p. 275.
[112] Dolphin, D.; Traylor, T. G.; Xie, L. Y. *Acc. Chem. Res*. **1997**, *30*, 251.
[113] (a) Penner-Hahn, J. E.; McMurray, T. J.; Renner, M.; Latos-Grazinsky, L.; Smith-Eble, K.; Davis, I. M.; Balch, A. L.; Groves, J. T.; Dawson, J. H.; Hodgson, K. O. *J. Biol. Chem*. **1983**, *258*, 12761. (b) Penner-Hahn, J. E.; Smith-Eble, K.; McMurray, T. J.; Renner, M.; Balch, A. L.; groves, J. T.; Dawson, J. H.; Hodgson, K. O. *J. Am. Chem. Soc*. **1986**, *108*, 7819.
[114] Shappacher, M.; Weiss, R.; Montiel-Montoya, R.; Trautwein, A.; Tabard, A. *J. Am. Chem. Soc*. **1985**, *107*, 3736.
[115] Antony, J.; Grodzicki, M.; Trautwein, A. X. *J. Phys. Chem. A* **1997**, *101*, 2692.
[116] Ghosh, A.; Almlöf, J.; Que, L. Jr. *J. Phys. Chem*. **1994**, *98*, 5576.
[117] Weiss, R.; Mandon, D.; Wolter, T.; Trautwein, A. X.; Müther, M.; Bill, E.; Gold, A.; Jayaraj, K.; Terner, J. *J. Biol. Inorg. Chem*. **1996**, *1*, 377.
[118] Sivaraja, M.; Goodin, D. B.; Smith, M.; Hoffman, B. M. *Science*, **1989**, *245*, 738.
[119] Morimoto, A.; Tanaka, M.; Takahashi, S.; Ishimori, K.; Hori, H.; Morishima, I. *J. Biol. Chem*. **1998**, *24*, 14753.
[120] Yamamoto, S.; Kashiwagi, H. *Chem. Phys. Lett*. **1988**, *145*, 111.
[121] Kuramochi, H.; Noodleman, L.; Case, D. A. *J. Am. Chem. Soc*. **1997**, *119*, 11442.
[122] Wirstam, M.; BLomerg, M. R. A. *J. Am. Chem. Soc*. **1999**, *121*, 10178.
[123] Collman, J. P.; Gagne, R. P.; Reed, C. A.; Robinson, W. T.; Rodley, G. A. *Proc. Natl. Acad. Sci. USA* **1976**, *71*, 1326.
[124] Stephens, P. J.; Devlin, F. J.; Chabalowski, C. F.; Frish, M. J. *J. Phys. Chem*. **1994**, *98*, 11623.
[125] Solar, J. P.; Mares, F.; Diamond, S. E. *Cat. Rev. Sci. Eng*. **1985**, *27*, 1.
[126] Guenguerich, F. P.; McDonald, T: L. *Acc. Chem. Res*. **1984**, *17*, 9.
[127] Cythocrome P-450, Structure, Mechanism and Biochemistry, Ortiz de Montellano, P. R. Ed.; Plenum Press, New York, 1986.
[128] Gunter, M. J.; Turner, P. *Coord. Chem. Rev*. **1991**, *108*, 115.
[129] Lichtenberg, F.; Nastainczik, W.; Ullrich, V. *Biochem. Biophys. Res. Commun*. **1976**, *70*, 939.
[130] Koola, J. D.; Kochi, J. K. *J. Org. Chem*. **1987**, *52*, 4545.

[131] Nam, W.; Valentine, J. S. *J. Am. Chem. Soc*. **1993**, *115*, 1772.
[132] Mukerjee, S.; Skogerson, K.; DeGala, S.; Caradonna, J. P. *Inorg. Chim. Acta* **2000**, *297*, 313.
[133] Groves, J. T.; Nemo, T. E.; Myers, R. S. *J. Am. Chem. Soc*. **1979**, *101*, 1032.
[134] (a) Macikenas, D.; Skrzypczak-jankun, W.; protasiewicz, J. D. *J. Am. Chem. Soc*. **1999**, *121*, 7164. (b) Macikenas, D.; Skrzypczak-Jankun, W.; Protasiewicz, J. D. *Angew. Chem. Int. Ed. Engl*. **2000**, *39*, 2007.

Apèndix
altres publicacions

Basis set influence on the ab initio description of the dihydrogen complex $[Os(PH_3)_2Cl(CO)H(H_2)]$ Barea, G.; Maseras, F.; Ujaque, G.; Lledós, A. *Journal of molecular Structure (Theochem)*, **1996**, *371*, 59.

Synthesis and characterization of $OsX\{NH=C(Ph)C_6H_4\}(P^iPr_3)_2$ (X=H, Cl, Br, I): nature of the H_2 unit and its behavior in solution. Barea, G.; Esteruelas, M.A.; Lledós, A.; López, A.M.; Oñate, E.; Tolosa, J.I. *Organometallics*, **1998**, *17*, 4065.

Synthesis and Spectroscopic and Theoretical Characterization of the longated Dihydrogen Complex $OsCl_2(h^2\text{-}H_2)(NH=CPh_2)(P^iPr_3)_2$. Barea, G.; Esteruelas, M.A.; Lledós, A.; López, A.M.; Tolosa, J.I. *Inorg. Chem*. **1998**, 37, 5033.

Thermally activated site exchange and quantum exchange coupling processes in unsymetrical trihydrido osmium compounds. Barea, G.; Castillo, A.; Esteruelas, M.A.; Lahoz, F.J.; Lledós, A.; Maseras, F.; Modrego, J.; Oñate, E.; Oro, L.A.; Ruiz, N.; Sola, E. *Inorg. Chem*. **1999**, 38, 1814.